Influence of Age and Frailty on Intestinal and Hepatic Bile Acid Transport in Male C57BL/6 Mice

by

Tiandai Gao

Submitted in partial fulfillment of the requirements

for the degree of Master of Science

at

Dalhousie University

Halifax, Nova Scotia

July 2016

TABLE OF CONTENTS

LIST OF TABLES

LIST OF FIGURES

Abstract

Bile acids regulate their own synthesis as well as glucose and lipid metabolism. Bile acid homeostasis is maintained in part by enterohepatic circulation, which requires the concerted activity of multiple transporters, namely the apical sodium-dependent bile acid transporter (ASBT) and organic solute transporter (OST) α/β in the ileum, and the Na^+-taurocholate cotransporting polypeptide (NTCP) and bile salt export pump (BSEP) in the liver. Limited data suggest that intestinal bile acid absorption decreases with aging, but this has never been measured experimentally. Age-related changes in the expression of bile acid transporters have also been described, albeit, the data are limited. Importantly, nothing is known about the influence of frailty on bile acid transport – frailty being defined as an increased vulnerability to adverse health outcomes. We hypothesized that intestinal bile acid absorption decreases with increasing age and frailty and that there is a decreased expression of transporters involved in enterohepatic bile acid circulation. Here we measured intestinal bile acid absorption in Ussing chambers and the mRNA expression by qPCR of ileal (Asbt, Ostα/β, Fgf15 and Fxr) and hepatic (Ntcp, Bsep, Fxr, and Cyp7a1) bile acid transporters and regulatory proteins as a function of age and frailty level in male C57BL/6 mice (89-953 days of age). A non-invasive frailty assessment was conducted on individual mice prior to experiments. There was a significant positive linear correlation between age and frailty index score (R^2=0.718, p<0.0001, n=21). The intestinal bile acid absorption rate decreased in a linear manner with both increasing age (R^2=0.383, p=0.006, n=18) and frailty index score (R^2=0.328, p=0.013, n=18). The intestinal bile acid absorption rate was 52% significantly lower in the older cohort of mice (mean age of 752 days old, n=12) compared to the younger cohort (mean age of 151 days old, n=9) (p=0.0006, unpaired two-tailed *t*-test). There was a modest decrease in the intestinal expression of Asbt, Ostα/β and Fxr with increasing age and frailty index score, which was not significant by linear regression analysis. However, the expression of Asbt was lower in the older compared to the younger cohort of mice (p=0.028, unpaired two-tailed *t*-test), but the expression of other genes did not differ between the two cohorts. There was also a modest decrease in the expression of the hepatic transporters as a function of increasing age and frailty index score. However, the only relationships that were significant were a negative linear correlation between age and Ntcp expression (R^2=0.265, p=0.017, n=19), and between age and Oatp1b2 expression (R^2= 0.274, p=0.015, n=21). Indeed, the expression of Ntcp and Oatp1b2 was significantly lower in the older compared to the younger cohort of mice (p=0.0125 and p=0.016, respectively). Together, these data indicated that intestinal bile acid absorption decreases with increasing age and frailty level. This effect is likely due to a decreased expression of intestinal bile acid transporters, Asbt and Ostα/β. The decrease in Ntcp and Oatp1b2 expression in older mice suggested that hepatic bile acid handling is also sensitive to age. Thus, enterohepatic circulation of bile acids likely diminishes with age and frailty, which could impact bile acid homeostasis, and pharmacokinetics and pharmacodynamics of drugs.

List of Abbreviations Used

^{3}H	Tritium
ASBT	Apical sodium-dependent bile acid transporter
Apo	Apolipoprotein
BSEP	Bile salt export pump
cAMP	Cyclic adenosine monophosphate
CAT	Carnitine acyltransferase
ChREBP	Carbohydrate-responsive element binding protein
CYP	Cytochrome P450
FGF	Fibroblast growth factor
FXR	Farnesoid X receptor
GLP-1	Glucagon-like peptide 1
GPBAR-1	G protein-coupled bile acid receptor 1
HDL	High-density lipoprotein
HEPES	Hydroxyethyl piperazineethanesulfonic acid
HMG-CoA	3-hydroxy-3-methyl-glutaryl-coenzyme A
HNF	Hepatic nuclear factor
IL	Interleukin
IP	Intraperitoneal
I_{sc}	Short-circuit current
LDL	Low-density lipoprotein
LRH	Liver receptor homolog

MRP	Multidrug resistance-associated protein
NTCP	Na^+-taurocholate cotransporting polypeptide
OATP	Organic anion-transporting peptide
OST	Organic solute transporter
PCSK9	Proprotein convertase subtilisin/kexin type 9
PPAR	Peroxisome proliferator-activated receptor
RAR	Retinoid acid receptor
RXR	Retinoid X receptor
TC	Taurocholate
TER	Transepithelial resistance
TNF	Tumor necrosis factor
TPD	Transepithelial potential difference
SHP	Small heterodimer partner
SREBP	Sterol regulatory element-binding protein
VLDL	Very low-density lipoprotein

ACKNOWLEDGEMENTS

I would like to first express my gratitude to my supervisor, Dr. Ryan Pelis, who offered me the chance to study in his lab and guided me throughout. He taught me many useful techniques and knowledge. More importantly, I learned the way of thinking as a researcher from him, which will benefit me greatly in the long term. He has always been so supportive and patient with me in every aspect. It would be impossible to finish the project without his expertise and encouragement. In addition, I would like to thank Dr. Kerry Goralski, Dr. Christian Lehmann, and Dr. Jason Berman, for all your valuable advice and support, as well as your effort in reviewing my thesis.

I would also like to thank Dr. Susan Howlett for providing us the experimental animals and exchanging her great idea with us. To Hirad Feridooni and Hailey Jansen, thanks for doing the frailty score and answering many questions from me.

A big thank you all the lab members, Adam Hotchkiss, Mansong Li, Leslie Ingraham, and Jonghwa Lee. You helped me with the project from the first day I started. Every one of you has been so helpful and friendly to me all the time. It's been a great pleasure to work and be friends with you. And to Jesslyn Kinney, Luisa Vaughan, and Sandi Leaf, thank you for making the administrative tasks a lot easier for me.

Finally, a special thank you to my family and friends. Your support and understanding have been really helpful all the time. I can't picture myself going through this two-year journey without any of you.

CHAPTER 1: INTRODUCTION

1.1 Bile Acids and Their Synthesis

1.1.1 Common bile acids in human

Bile acids are water-soluble, amphipathic molecules that are synthesized from cholesterol. There are two major classes of bile acids – primary bile acids and secondary bile acids. Primary bile acids are synthesized by the liver whereas secondary bile acids are generated from the metabolism of primary bile acids by bacteria in the colon. In human, cholic acid and chenodeoxycholic acid are the primary bile acids, while deoxycholic acid and lithocholic acid are the secondary bile acids (1). Most bile acids are conjugated to taurine or glycine in hepatocytes (1). Human bile consists mostly of conjugates of cholic acid, chenodeoxycholic acid, and deoxycholic acid, whereas only trace amount of conjugated lithocholic acid is present (2). **Table 1.1** shows the chemical structures of bile acids, and their glycine and taurine conjugates.

1.1.2 Biochemistry of bile acid synthesis

The detailed biochemistry of bile acid synthesis is beyond the scope of this thesis, and therefore, I will only mention some fundamental concepts regarding the process. Daily synthesis of bile acids is estimated to be approximately 0.5 grams, which roughly replaces the daily fecal loss of bile acids (3). The synthesis of primary bile acids takes place in the liver, using cholesterol as the substrate. Two main pathways account for most of the bile acid synthesis, namely the “classical” pathway and the “alternative” pathway (4). It is estimated that, in mice, the classical pathway contributes 75% to the bile acid pool while the alternative pathway accounts for the remaining 25% (5). The four major steps in primary bile acid synthesis are

initiation, modification of the ring structure, oxidation, and shortening of the side chain followed by conjugation (3). The steps in bile acid synthesis are discussed below.

Initiation: In the classical pathway, cholesterol is converted to 7-hydroxycholesterol by CYP7A1 (aka, cholesterol-7α-hydroxylase), a microsomal cytochrome P450 enzyme. CYP7A1 is the rate-limiting enzyme in the classical pathway of bile acid synthesis. Several alternative pathways exist. The most notable one is the sterol 27-hydroxylase pathway, which involves cytochrome P450 enzyme 27A1 (CYP27A1, aka, sterol 27-hydroxylase) and CYP7B1 (aka, oxysterol 7α-hydroxylase). The 27-hydroxylase pathway contributes ~9% to the bile acid pool in human (6). Other minor alternative pathways are initiated by cholesterol 24-hydroxylase and cholesterol 25-hydroxylase (3).

Modification of ring structures: After initiation in the classical and alternative pathways, the intermediates are 7α-hydroxylated and undergo modification of their side rings. The first step involves the conversion of the 7α-hydroxylated form into the 3-oxo, Δ4 form by microsomal 3β-hydroxyl-Δ^5-C_{27}-steroid oxidoreductase (C_{27} 3β-HSD) (3). The product of C_{27} 3β-HSD metabolism undergoes one of two routes in subsequent steps. The route with CYP8B1 (sterol 12α-hydroxylase) ultimately leads to the synthesis of cholic acid, whereas the route without CYP8B1 results in chenodeoxycholic acid synthesis (3).

Oxidation and shortening of the side chain: the products of ring structure modification subsequently undergo oxidation and side chain shortening. The first several steps require CYP27A1, the enzyme involved in the initiation of bile acid synthesis in the alternative pathway. After multiple steps involving various enzymes, cholyl-CoA and chenodeoxycholyl-CoA are made (3).

Conjugation: The final step in bile acid synthesis is the addition of taurine or glycine to carbon 24, replacing the Coenzyme A. The reaction is catalyzed by bile acid-CoA: amino acid N-acyltransferase. This reaction is so efficient that 98% of bile acids secreted from the liver are conjugated (3). Conjugated bile acids are secreted into bile faster than unconjugated bile acids (7). Conjugation increases the water solubility and amphipathicity of bile acids, rendering bile acids relatively impermeable to cell membranes, thus enhancing their emulsifier function (8).

1.1.3 Regulation of bile acid synthesis

Bile acid synthesis is regulated by bile acids themselves as well as cholesterol and some hormones. Bile acid synthesis is under tight regulation in order to maintain proper bile acid levels, in particular, to prevent cytotoxicity caused by exposure to high concentrations of bile acids. To follow is a discussion of the effect of bile acids on their own *de novo* synthesis. The expression of the rate-limiting enzyme of the classical pathway, CYP7A1, is suppressed by bile acids, through a negative feedback regulatory mechanism (9, 10). In addition, the expression of CYP8B1 is also downregulated by bile acids (11). Farnesoid X receptor (FXR) is a bile acid nuclear receptor (12). The downregulation of CYP7A1 and CYP8B1 is primarily accomplished through two pathways involving FXR – namely the FXR/SHP and FXR/FGF19/FGFR4 pathways. **Figure 1.1** shows the two major pathways that regulate bile acid synthesis. The FXR/SHP pathway occurs in hepatocytes. Upon activation by bile acids, FXR induces the expression of small heterodimer partner (SHP). SHP subsequently inhibits the activity of liver receptor homolog-1 (LRH-1), resulting in suppression of CYP7A1 and CYP8B1 gene transcription (13, 14). In addition, SHP also acts on hepatic nuclear factor 4α (HNF4α), leading to suppression of CYP7A1 and CYP8B1 gene transcription (15, 16). The FXR/FGF19/FGFR4 pathway occurs in epithelial cells of the ileum, where activation of Fxr by bile acids induces the

expression of fibroblast growth factor 15 (Fgf15 is the mouse ortholog of human FGF19). Fgf15 is a secreted protein that travels from the intestine to the liver through the portal vein system or lymph. Fgf15 subsequently binds the Fgf receptor 4 (Fgfr4) on the hepatocyte membrane, resulting in suppression of Cyp7a1 expression (17). The FXR/FGF19/FGFR4 pathway also functions in a paracrine manner, where bile acids in hepatocytes bind FXR, inducing the expression of FGF19, which is then secreted and activates FGFR4 on neighboring hepatocytes to suppress CYP7A1 expression (18).

Taken together, bile acids suppress their own production via two FXR-dependent pathways, with the two pathways leading to the suppression of CYP7A1 and CYP8B1 expression. However, studies in mice suggested that the two pathways may differentially regulate CYP7A1 and CYP8B1 expression. The basal expression of Cyp7a1 is not altered in liver-specific Lrh-1 knockout mice, and the repression of Cyp7a1 expression by Fxr remains intact in these mice (19), while the basal expression of Cyp8b1 is lower in liver-specific Lrh-1 knockout mice, and there is a corresponding change in the bile acid pool composition in these mice (19, 20). Furthermore, liver-specific Fxr deficiency in mice attenuates the repression of Cyp8b1 by synthetic FXR agonist treatment (21). On the other hand, mice treated with recombinant Fgf15 have decreased levels of Cyp7a1 expression whereas there is no change in Cyp8b1 expression (21). These findings suggest that the expression of Cyp7a1 is more dependent on the Fxr/Fgf15/Fgfr4 pathway, whereas the expression of Cyp8b1 is more dependent on the Fxr/Shp pathway.

1.2 Bile Acid Enterohepatic Circulation and Bile Acid Transporters

1.2.1 Enterohepatic circulation

Enterohepatic circulation of bile acids is a highly efficient process involving the concerted activity of several intestinal and hepatic bile acid transporters. Bile acids are secreted into the bile canaliculi by transporters in the canalicular (apical) membrane of hepatocytes for subsequent storage in the gallbladder. After meal consumption, the gallbladder contracts and bile acids are released into the duodenum, and most of this bile acid load (approximately 95%) is actively absorbed by transporters in the terminal ileum (22). The remainder of primary bile acids enter the colon where they are transformed into secondary bile acids, and some secondary bile acids are also absorbed by the colon (22). Bile acids in the intestinal epithelial cells then move across the basolateral membrane via facilitated diffusion, thus entering the portal circulation where they are subsequently taken up by transporters on the sinusoidal (basolateral) membrane of hepatocytes (22). In human, approximately 3 g of bile acids undergo enterohepatic circulation 4-12 times/day, and the bile acids lost in feces (approximately 200-600 mg) are replenished by *de novo* synthesis in the liver (23). **Figure 1.2** shows the transporters involved in the enterohepatic circulation of bile acids.

1.2.2 Intestinal bile acid transporters

The terminal ileum is the major site of intestinal bile acid absorption. The apical sodium-dependent bile acid transporter (ASBT) actively transports bile acids from the lumen of the terminal ileum into the intestinal epithelial cell. Bile acids are then transported across the basolateral membrane into the portal vein circulation by the organic solute transporter dimer α/β (OST α/β). This transepithelial transport process is extremely efficient with ~95% of the bile acid load secreted from the gallbladder being absorbed into the hepatic portal circulation.

ASBT (SLC10A2)

ASBT is expressed in the apical membrane of epithelial cells of the terminal ileum, where it transports bile acids from the intestinal lumen into the epithelial cells (24). The transporter is also expressed in cholangiocytes and renal proximal tubule cells (25, 26). Bile acid enterohepatic circulation is eliminated in Asbt knock-out mice, highlighting the importance of Asbt in enterohepatic bile acid circulation (27). ASBT transports bile acids in a strictly Na^+-dependent manner, with a stoichiometry of one bile acid per two Na^+ ions (28). Thus, the Na^+ gradient and negative intracellular membrane potential, established in part through the activity of Na^+, K^+-ATPase, energize bile acid transport by ASBT (28). ASBT has a narrow substrate selectivity, transporting almost exclusively monovalent bile acids (29).

OST α/β (SLC50A/B)

OSTα and OSTβ are two independent proteins that form a dimer capable of transporting bile acids (30). Ostα and Ostβ mRNA expression are detected in mouse ileum and kidney, which mirror the cellular expression pattern of Asbt (31). Ostα/β localizes to basolateral membranes in intestinal epithelial cells (31). OSTα/β exhibits broad substrate selectivity *in vitro*, transporting organic solutes such as estrone sulfate, digoxin, prostaglandin E_2 and bile acids (30). Bile acid transport by Ostα/β is Na^+-independent and occurs via facilitated diffusion driven by the electrochemical gradient of bile acids (31). Studies with Ostα-null mice confirmed the essential role of Ostα/β in basolateral membrane transport of bile acids. That is, Ostα-null mice exhibited a dramatic decrease in intestinal bile acid absorption and the size of their bile acid pool (32).

1.2.3 Hepatic bile acid transporters

Bile acids absorbed by the intestine travel to the liver via the portal vein circulation. In the liver, the uptake of conjugated bile acids is mediated mainly by Na^+-dependent transport, whereas the uptake of unconjugated bile acids is mediated mainly by Na^+-independent transport

(33). The Na^+-taurocholate cotransporting polypeptide (NTCP) accounts for most of the Na^+-dependent uptake of conjugated bile acids (34), and several members of the organic anion transporting peptide (OATP) family are responsible for the Na^+-independent uptake of unconjugated bile acids (35, 36). Following their uptake across the basolateral (sinusoidal) membrane into hepatocytes, bile acids are effluxed across the canalicular membrane into the bile canaliculi by the bile salt export pump (BSEP), in spite of a steep opposing bile acid concentration gradient (37). Several other transporters are also involved in the export of bile acids from hepatocytes, including multidrug resistance-associated protein (MRP) 3 and MRP 4 (38, 39). These transporters are expressed on the basolateral membrane of hepatocytes. They are not the major bile acid efflux transporters under normal conditions, but their expression can be induced during cholestasis (40, 41), protecting the hepatocytes from bile acid cytotoxicity and shifting bile acids to renal elimination (22).

NTCP (SLC10A1)

The expression of NTCP is limited to the sinusoidal membrane of hepatocytes (42), and its activity accounts for most of the Na^+-dependent bile acid uptake into hepatocytes (43). NTCP is structurally and functionally similar to ASBT. NTCP shares 35% and 63% amino acid identity and similarity, respectively, with ASBT (44). NTCP uses a strictly Na^+-dependent cotransport mechanism with a stoichiometry of two Na^+ ions to one bile acid, similar to that of ASBT (45) Like ASBT, NTCP is energized by the Na^+ gradient and inside negative membrane potential (46). In spite of their similarities, NTCP has a broader substrate selectivity than ASBT (29), with both conjugated and unconjugated bile acids as substrates, although the transporter interacts preferentially with conjugated bile acids (43). NTCP also transports various endogenous

steroids, small molecule drugs, and possibly drugs that are covalently bound to conjugated bile acids (47).

BSEP (ABCB11)

An ATP-dependent bile acid secretory system (cellular efflux transport via ATP hydrolysis) was initially identified in the canalicular membrane of rat hepatocytes (48). The Bsep (formerly named as a sister of p-glycoprotein, sPgp) gene was cloned from liver and its function as an ATP-dependent bile acid efflux transporter was confirmed (49, 50). BSEP expression is limited to the canalicular membrane of hepatocytes, and in this locale, it is involved in transporting bile acids from the cell into the bile canaliculi (50). BSEP has a high affinity for conjugated bile acids (51), but low affinity for unconjugated bile acids (52). A central role for BSEP in the biliary secretion of bile acids was established by the fact that mutation of BSEP in humans leads to progressive familial intrahepatic cholestasis 2 (53).

1.3 Regulation of Bile Acid Transporters

Similar to the key enzymes in bile acid synthesis (CYP7A1 and CYP8B1), intestinal and hepatic bile acid transporters are regulated primarily at the transcriptional level by bile acids working through FXR. In many cases, the signaling molecules downstream of FXR that regulate CYP7A1 and CYP8B1 expression (SHP, LRH-1, FGF19, and FGFR4) are the same as those that regulate bile acid transporters. Bile acid transporters are under regulation in order to maintain proper enterohepatic circulation of bile acids and to protect the intestinal epithelial cells and hepatocytes from toxicity associated with increased intracellular bile acid concentration. **Figure 1.3** shows the change in expression level (increase or decrease) of ASBT, OSTα/β, NTCP and BSEP with elevated levels of bile acids. There are also other factors, such as hormones, that regulate bile acid transporter expression. Discussion of these other factors will be limited.

1.3.1 Regulation of intestinal bile acid transporters

ASBT

Since ASBT is involved in intestinal bile acid absorption, increased levels of bile acids are expected to cause a decrease in ASBT expression, as highlighted from the studies below. Studies in mice and rabbits indicate that bile acids suppress the expression of Asbt via the Fxr/Shp pathway (54). In a human *in vitro* study, bile acids activated FXR, leading to an increase in the expression of SHP (55). SHP, in turn, reduced the activity of RXRα: RARα (retinoid X receptor α: retinoid acid receptor α), which led to decreased ASBT expression (55). A recently proposed mechanism involves the FXR/FGF19/FGFR4 pathway, where FGF19 binds to the FGFR4 receptor on the basolateral membrane of intestinal epithelial cells, causing a decreased ASBT expression (56).

OSTα/β

Exogenous bile acid administration and administration of FXR agonists increase the expression of Ostα and Ostβ (57-59). Since OSTα/β are involved in bile acid efflux from intestinal epithelial cells, the upregulation of the dimer with elevated bile acid levels and FXR activation likely protect the epithelial cells from high intracellular levels of bile acids. The Ostα and Ostβ promoters contain both Fxr and Lrh-1 response elements. The activation of Fxr leads to increased Ostα and Ostβ promoter activity and increased Ostα/β expression (57). Also, the upregulation of Ostα and Ostβ expression by bile acid feeding is eliminated in Fxr-null mice (59). In terms of Lrh-1, expression of Lrh-1 increased Ostα and Ostβ promoter activity, and the promoters' activity decreased with the co-expression of Shp (57). Accordingly, basal Ostα and Ostβ promoter activity are reduced in mice with a mutation in Lrh-1 response element or mice with decreased Lrh-1 expression (57). The effect of Fxr activation on Ostα/β expression has

been proposed as follows: bile acids activate Fxr to induce the expression of Ostα/β. However, Fxr activation also causes increased expression of Shp, which inactivates Lrh-1 thus reducing the expression of Ostα/β (57). Though both positive and negative regulation of Ostα/β is apparent, the positive regulation by Fxr is thought to dominate, thereby limiting the potential cellular toxicity caused by overexposure to bile acids (57).

1.3.2 Regulation of hepatic bile acid transporters

NTCP

As anticipated, elevated bile acid levels in the body caused reduced expression of the major hepatic bile acid uptake transporter NTCP. Bile acids suppress the transcription of NTCP in a complex pattern involving FXR. In the rat, upon activation by bile acids, Fxr induces the expression of Shp (60). Shp, in turn, prevents the nuclear receptor, Rxrα:Rarα, from binding to the Ntcp transcription promoter and activating Ntcp transcription (60). Shp also interacts with Hnf-4α, resulting in decreased activation of Hnf-1α, which normally activates Ntcp transcription in the rat (61). Hnf-4α directly activates Ntcp expression in the mouse, and Ntcp expression is greatly decreased in Hnf-4α knockout mice (15). However, HNF-4α, HNF-1α, and RXRα: RARα do not interact with the human NTCP promoter (61). In addition, Ntcp expression was reduced in Shp-null mice fed a cholic acid diet (62). These findings suggest that other mechanisms may be at play.

BSEP

Elevated intracellular bile acids lead to increased expression of BSEP (26). The regulation of BSEP transcription is directly mediated by FXR (63). That is, upon activation by bile acids, FXR forms a heterodimer with the nuclear receptor, RXRα. The FXR: RXRα heterodimer effectively binds to the BSEP gene promoter and activates its transcription (63).

This direct regulation is further supported by the fact that Fxr-null mice do not show increased Bsep expression upon bile acid feeding (64).

1.3.3. Other factors regulating intestinal and hepatic bile acid transporters

The ASBT promoter has peroxisome proliferator-activated receptor (PPAR) α and Vitamin D receptor response elements, and binding of both cause an increase in ASBT transcription (65, 66). Glucocorticoids induce the expression of ASBT in the ileum by activating the glucocorticoid receptor, which increases the activity of the ASBT gene promoter (67). Intestinal inflammation also affects the expression of ASBT. Individuals with Crohn's disease have lower ASBT expression levels than healthy individuals (67).

The expression of NTCP and BSEP are modulated by the immune response and hormones. The expression of NTCP is rapidly downregulated by lipopolysaccharide and multiple pro-inflammatory cytokines such as IL-1, IL-6, and TNF-α (68, 69). Interestingly, sepsis is associated with cholestasis (70), and lipopolysaccharide treatment of rat liver reduces the expression of Bsep, which could contribute to cholestasis (71). Another study showed that following lipopolysaccharide treatment, there was a relocation of Bsep from the canalicular membrane to pericanalicular membrane vesicle compartment (72). Growth hormone and glucocorticoids increase NTCP expression (73, 74), whereas estrogen decrease the expression of NTCP (75).

The expression of BSEP is also regulated by Vitamin A. In an *in vitro* study, Vitamin A disrupted the binding of the FXR: RXRα heterodimer to the BSEP promoter thus attenuating the induction of BSEP transcription by FXR agonists (76). Indeed, Vitamin A strongly eliminates bile acid-induced BSEP expression, and Vitamin A deficiency plus cholic acid administration results in a high level of Bsep expression *in vivo* in mice (77).

The activity of NTCP and BSEP are also subject to acute regulation. For example, an increase in intracellular cAMP increases the translocation of Ntcp to the sinusoidal membrane (78). Treatment of rats with bile acid or bucladesine (a cAMP analog) resulted in a rapid increase of Bsep insertion into the canalicular membrane, and the increase was diminished by colchicine, confirming the presence of an intracellular vesicular pool of Bsep (79, 80). The rapid regulation of BSEP translocation is thought to be a response of the hepatocyte to the postprandial increase in bile acid influx across the membrane (81).

1.4 Metabolic Effects of Bile Acids

A well-established physiological role of bile acids is in the digestion of dietary fat through emulsification (82). Other physiological functions include the elimination of cholesterol and stimulation of bile flow (2). More recently, there is an interest in the ability of bile acids to regulate glucose, lipid, and energy metabolism – a topic on which I focus in the following sections. The effects of bile acids on metabolic processes are predominantly mediated by FXR and a G-protein coupled receptor called TGR5 (aka, G protein-coupled bile acid receptor 1, GPBAR-1) (83).

1.4.1 FXR regulation of glucose metabolism

Bile acids acting through FXR modulates insulin secretion by pancreatic β-cells, peripheral insulin sensitivity, and gluconeogenesis. FXR is expressed in human pancreatic β-cells and its activation stimulates glucose-induced insulin transcription and secretion (84). In non-obese diabetic mice, Fxr activation stimulates insulin secretion and hepatic glucose uptake and delays the development hyperglycemia, glycosuria, and diabetes (84). Compared to wild-type mice, Fxr-null mice exhibit signs of insulin resistance, such as hyperglycemia, elevated blood glucose after a glucose tolerance test, and a lower whole-body blood glucose disposal (85-

87). There is also evidence that the response of peripheral tissues to insulin is impaired in Fxr-null mice at the molecular level (86, 87). Fxr activation by bile acids represses the expression of several enzymes involved in gluconeogenesis, including phosphoenolpyruvate carboxykinase, glucose-6-phosphate, and fructose-1, 6-bisphosphatase (88). Fxr decreases the expression of these enzymes in a Shp-dependent fashion, with involvement from multiple other downstream nuclear receptors (88, 89). **Figure 1.4** shows the major regulatory effects of FXR on glucose metabolism.(88, 89).

Besides the FXR-SHP pathway, there is evidence that the FXR/FGF19/FGFR4 pathway may also regulate glucose metabolism. In human, the postprandial increase in plasma FGF19 levels tracks the increase in serum bile acid levels (90). FGF19 reduces the expression of enzymes involved in hepatic gluconeogenesis (91) and stimulates glycogen synthesis (92). However, there is some controversy on whether the effects of FGF19 are mediated through the FGFR4 receptor. In one study, Fgfr4-null mice were insulin resistant and hyperglycemic in glucose tolerance tests (93), but not in another study (94).

1.4.2 FXR regulation of cholesterol metabolism

Cholesterol is required for bile acid synthesis, and bile acid synthesis is a major pathway for eliminating cholesterol from the body. Studies suggest that bile acids working through FXR are beneficial in reducing low-density lipoprotein cholesterol (LDL-C), a complex linked to the development of atherosclerosis. Activation of Fxr by bile acids or synthetic Fxr agonists causes a reduction in total cholesterol in a diabetic mouse model, and Fxr-null mice show an increase in plasma LDL-C (95). The mechanism by which FXR activation causes a reduction in plasma LDL-C levels has been attributed to the suppression of proprotein convertase subtilisin/kexin type 9 (PCSK9). PCSK9 is a protease that increases the degradation of the low-density

lipoprotein receptor (LDLR), a receptor that mediates cellular LDL internalization thus clearing LDL from the circulation (96). Human hepatocytes treated with chenodeoxycholic acid or a synthetic FXR agonist showed a decrease in PCSK9 gene expression, and co-administration of chenodeoxycholic acid with a statin further potentiated the effect of the statin on increasing LDLR activity (97). Monoclonal antibodies that target PCSK9 for degradation exhibit promising safety and efficacy profiles over other newer LDL-lowering strategies (96). Thus, suppression of PCSK9 expression via modulation of FXR may be a potential adjuvant therapy to statins.

Given a link between FXR and LDL-C levels, and the relationship between LDL-C levels and atherosclerosis, FXR activity and the development of atherosclerosis could be associated. Many of the studies examining the role of FXR in atherosclerosis development used Fxr-knockout mice in combination with Apoe-knockout or Ldlr-knockout. Apoe-knockout or Ldlr-knockout mice display increased susceptibility to atherosclerosis (98). One study showed that Fxr-null/Apoe-null mice have larger atherosclerotic lesions in their aortas than Apoe-null mice (99). Fxr-null/Apoe-null mice also had increased LDL-C and decreased HDL-C, and marked lipid accumulation in the liver compared to Apoe-null mice (99). However, atherosclerosis did not happen in Fxr-null mice, despite the fact that Fxr deficiency alone led to marked lipid accumulation in the liver (99). Apoe-null or Ldlr-null mice treated with a synthetic Fxr agonist had fewer atherosclerotic lesions, supporting a role for Fxr in reducing the incidence of atherosclerosis (98, 100). Interestingly, bile acid sequestrants, namely cholestyramine and colesevelam, reduce serum LDL-C levels and are associated with a decreased risk of coronary artery disease (101).

1.4.3 FXR regulation of triglyceride metabolism

FXR activation lowers serum triglyceride levels by decreasing hepatic triglyceride production, increasing hepatic triglyceride oxidation, and increasing peripheral triglyceride clearance, as discussed below. **Figure 1.5** shows the regulatory effects of FXR in triglyceride homeostasis. The sterol regulatory element binding protein (SREBP)-1c is a transcription factor that binds to gene promoters containing steroid response elements and activates their transcription (102). SREBP-1c increases the transcription of multiple enzymes involved in triglyceride synthesis, thus elevating triglyceride levels (103). In a mouse model of hypertriglyceridemia, hepatic triglyceride accumulation, VLDL secretion, and serum triglyceride levels are reduced following Fxr activation by cholic acid, and cholic acid feeding decreased hepatic expression of SREBP-1c and its lipogenic target genes (104). Carbohydrate-responsive element binding protein (ChREBP) is another transcription factor that is involved in triglyceride synthesis. ChREBP induces the expression of hepatic lipogenic and glycolytic genes (105). FXR interacts directly with ChREBP to inhibit its activity, resulting in reduced gene expression of enzymes involved in lipogenesis and glycolysis (105). In summary, FXR activation causes reduced expression of SREBP-1c and reduced activity of ChREBP to reduce triglyceride synthesis.

The peroxisome proliferator-activated receptor (PPAR) α regulates triglyceride metabolism through an FXR-dependent mechanism. Upon activation, FXR binds to the FXR response element in the PPARα promoter and stimulates its transcription (106). The PPARα, in response to PPARα agonists, stimulates the production of carnitine acyltransferase I (CAT-I) (106). CAT-I catalyzes the first step in fatty acid β-oxidation. Thus, FXR activation may lower plasma triglycerides by increasing fatty acid oxidation.

The peripheral clearance of triglycerides is accomplished by apolipoprotein CII (apoCII), which is a component of very low density lipoproteins. ApoCII activates lipoprotein lipase on endothelial cells thus increasing the rate of triglyceride clearance from blood (107). Fxr increases the hepatic expression of apoCII, which leads to increased peripheral clearance of triglycerides and a decreased plasma triglyceride level (107).

1.4.4 TGR5 regulation of energy metabolism and blood glucose levels

In addition to FXR, bile acids are also ligands of TGR5, a membrane-bound G-protein coupled receptor whose signaling is coupled to cAMP (108). Secondary bile acids appear to be more potent ligands of TGR5 than primary bile acids (109). TGR5 is widely expressed in human tissues, examples include the spleen, intestine (mainly ileum and colon), pancreas, adipose tissue, liver sinusoidal endothelial cells, gallbladder epithelium, cholangiocytes and Kupffer cells (109-113). One function of TGR5 is to regulate energy expenditure. Activation of Tgr5 by bile acids increases the activity of type 2 iodothyronine deiodinase in brown adipose tissue of mice (114). Type 2 iodothyronine deiodinase converts thyroxine to triiodothyronine, which is a potent stimulator of energy expenditure (114). These mice show a reduced body weight gain and increased energy expenditure in brown adipose tissue (114).

TGR5, acting through glucagon-like peptide-1 (GLP-1), functions to lower blood glucose levels. The effect of Tgr5 activation on Glp-1 release was first studied using an endocrine cell line called STC-1, which expresses Tgr5. In STC-1 cells, activation of Tgr5 by bile acids promotes the secretion of Glp-1 (115). Glp-1 is an incretin that stimulates insulin release from pancreatic β-cells (116). When Tgr5 was overexpressed in mice, there was an increase in intestinal Glp-1 release resulting in lower plasma glucose levels following an oral glucose challenge test (117). Similarly, another study showed that a synthetic Tgr5 agonist induced Glp-

1 release, and lowered plasma glucose in an oral glucose challenge test in an obese mouse model (118). These data suggest that TGR5 signaling is critical in regulating intestinal GLP-1 secretion and glucose homeostasis *in vivo*. More recently, another mechanism by which TGR5 regulates glucose metabolism has been proposed. Activation of Tgr5 in pancreatic β-cells stimulates insulin secretion (119) via a cAMP/PKA-dependent pathway (120).

1.4.5. ASBT inhibitors for the treatment of type II diabetes

There has been a recent interest in designing small molecule drugs that inhibit intestinal ASBT for the treatment type II diabetes. The mechanism proposed involves TGR5 and GLP-1 in the intestine. Indeed, oral administration of an Asbt inhibitor, 264W94, to diabetic rats led to increased plasma Glp-1, lower fasting plasma glucose levels and HbA1C levels, and a lower plasma glucose level following an oral glucose challenge test (121). ASBT is mainly expressed on the apical membrane of epithelial cells of the ileum, whereas TGR5 is expressed in the ileum as well as the colon (113). Though activation of Tgr5 by bile acids in the ileum appears to be a post-absorption process that is dependent on Asbt-mediated bile acid transport , bile acid absorption in the colon is predominantly dependent on passive diffusion (122). Presumably, inhibition of ASBT in the ileum leads to increased delivery of bile acids to the colon where their passive absorption makes them available for interaction with TGR5 at the basolateral side of the tissue. Treatment of colonic L-cells with bile acids causes them to increase their secretion of Glp-1 (121, 123). Recently, a highly potent, non-absorbable ASBT inhibitor, GSK2330672, was developed and shows excellent pharmacological properties for treatment of type 2 diabetes and clinical developability (124).

1.5 Pharmacokinetics and Bile Acid Transporters

In addition to performing an important physiological role in enterohepatic bile acid cycling, limited evidence suggests that bile acid transporters are pharmacologically important as well – some evidence was already presented (ASBT inhibitors and type II diabetes). Many of the bile acid transporters also transport drugs, and there is some evidence that they may influence the pharmacokinetics of their drug substrates. Also, there is an intense investigation on 'high-jacking' intestinal bile acid transporters in order to increase oral bioavailability, and hepatic bile acid transporters in order to target drugs specifically to the liver (125). In particular, a strategy has been to conjugate bile acids to drugs, making them amenable to transport by bile acid transporters, and subsequently taking advantage of metabolism to convert the drug to its active form, i.e., pro-drug strategy.

1.5.1 Bile acid transporters as drug transporters

Compared to other bile acid transporters, NTCP has a relatively broad substrate selectivity. A variety of drugs are NTCP inhibitors, including propranolol, progesterone, cyclosporine, bumetanide, furosemide, irbesartan, ezetimibe, as well as many others (126). On the other hand, some compounds, such as lidocaine, quinidine, and bupivacaine stimulate NTCP transport (126) (127). The ability of NTCP to interact with selected drugs suggests that it could be important for hepatic drug uptake, and inhibitors or stimulators of the transporter could influence hepatic elimination of some drugs.

BSEP has been shown to transport a limited number of drugs, such as pravastatin (128). Inhibition of BSEP by certain drugs may lead to cholestasis (37). Cyclosporine A, glybenclamide, rifampicin, and rifamycin are competitive BSEP inhibitors (51, 129). Other drugs that inhibit BSEP include bosentan, troglitazone and fluvastatin, and these drugs can cause acquired cholestasis, which rapidly resolves after cessation of drug therapy (37).

1.5.2 Bile acid-drug conjugate examples

HMG-CoA reductase inhibitors (statins): Statins are the first-line lipid management therapy for both primary and secondary prevention of cardiovascular disease (130). However, statins can cause side effects due to their inhibition of HMG-CoA reductase in extra-hepatic tissues, for example, myopathy (131). In one study, bile acid-statin conjugate showed that the conjugate was taken up preferentially into hepatocytes, where it was converted to its parent form, resulting in liver-specific inhibition of HMG-CoA reductase inhibition (132).

Cisplatin: Cisplatin is a platinum-based chemotherapeutic drug, which has multiple toxicities, such as nephrotoxicity. A bile acid-cisplatin conjugate called Bamet-UD2 was developed to target cisplatin to the liver, and tested for efficacy against liver tumors both *in vitro* and *in vivo* (133, 134). The anti-tumor effect of Bamet-UD2 was similar to that of cisplatin *in vitro* (133). A subsequent animal study showed that Bamet-UD2 had a lower systemic toxicity when treating liver tumors (134). Colon cancer and polyp cells express ASBT and several OATPs, and it was suggested that bile acid-chemotherapeutic conjugates such as Bamet-UD2 could be a favorable strategy for managing colon cancer (135).

Acyclovir: Acyclovir is a widely used antiviral drug with low oral bioavailability (~20%) (136), making intravenous administration often the only viable route for treatment of viral infections. An acyclovir-valylchenodeoxycholate conjugate was synthesized and shown *in vitro* to be transported with high affinity by ASBT (137), with cells expressing ASBT exhibiting a 16-fold higher uptake of acyclovir-valylchenodeoxycholate compared to acyclovir alone (137). Oral administration of acyclovir-valylchenodeoxycholate to mice resulted in a 2-fold increase in acyclovir bioavailability compared to administration of acyclovir alone (137). These findings

suggest that the oral bioavailability of acyclovir can be increased by taking advantage of ASBT transport with a bile acid-acyclovir conjugate.

1.6 The Concept of Frailty and the Effect of Age and Frailty on Bile Acid Homeostasis

The health status of individuals varies from fit to frail, so chronological age does not necessarily reflect the overall health status of an individual (138). The concept of frailty was introduced to account for the relationship between health status and clinical outcomes in elderly individuals. Frailty is defined as an increased vulnerability to adverse health outcomes, such as falls, delirium, and disability (139). The pathophysiology of frailty involves deficits in multiple organs and systems, such as the brain, endocrine system, immune system, musculoskeletal system, respiratory system, and cardiovascular system (139). There are multiple approaches to quantify frailty in human, one of which is the "frailty index" approach (140, 141). A human frailty index is a numerical measure of the number of health deficits in an individual and is based on clinical signs and laboratory abnormalities, where the deficits are counted and divided by the total number of possible deficits (142, 143). It should be noted that the number of deficits is more predictive of frailty than abnormalities in any particular system (144). In a large clinical study, a frailty index consisting of 92 variables was strongly correlated with a risk of death (145). Subsequent data analysis showed that the predictive validity could be preserved when the number of variables were reduced from 92 to 30 (145). The frailty index approach has been modified and extrapolated for use in mice, allowing for the study of the influence of frailty on biological processes (146). Initially, a method that involved invasive tests and specialized equipment was used to quantify frailty index in mice (147). However, its invasive nature and its need for specialized equipment limited its widespread use (147). To overcome this issue, a non-

invasive frailty index was developed for mice, which is based on an assessment of 31 variables (148) (see "Materials and Methods").

There is some limited evidence that bile acid homeostasis changes with age, but virtually nothing is known about the effects of frailty on mechanisms regulating bile acid homeostasis. Age-related changes in plasma bile acid profiles have been observed in healthy humans (149, 150). In an early study in rats, no age-related changes were detected in the biliary secretion of bile acids, the plasma bile acid pool size, the distribution of bile acids in the gastrointestinal tract, or bile acid turnover frequency (151). The most remarkable age-related change was in serum bile acid composition, where cholic acid levels increased while β-muricholic acid (derived from chenodeoxycholic acid) levels decreased with aging (151). A more recent study with mice showed that serum total bile acid concentration increased three-fold in female mice from 3 to 27 months old, whereas it remained relatively constant in male mice (152).

Age-related changes in bile acid enterohepatic circulation have been studied. Fasting serum levels of conjugated and unconjugated bile acids were similar in young (37 years old on average) and older (67 years old on average) humans (153). However, the postprandial serum level of conjugated bile acids was significantly lower in older subjects (153). This finding suggests that the absorption of conjugated bile acids becomes impaired with aging, and this is consistent with a study showing increased fecal bile acid levels with increasing age (154).

The change in expression of bile acid transporters and some other related genes has also been studied as a function of age, with apparent gender differences and some controversies between studies. The mRNA expression of Ntcp and Bsep remained relatively stable from 3 to 27 months of age in male mice (152). Whereas in female mice, Ntcp and Bsep levels increased from 3 to 9 months then decreased from 9 to 27 months (152). However, in another study, the

expression of Ntcp and Bsep was significantly lower in 24-month-old male mice compared to 12-month-old male mice (155). The mRNA expression of Oatp1b2 remained constant in male mice during aging, while it increased from 3 to 12 months and then decreased thereafter in female mice (152). While in another study, Oatp1b2 expression was significantly lower in 24-month-old male mice compared to 12-month-old male mice (155). The ileal bile acid transporters (Asbt and Ostα/β) remained relatively unchanged with age in both male and female mice (152). The expression of Cyp7a1 increased approximately two-fold from 3 to 18 months and decreased thereafter in male mice (152). In female mice, Cyp7a1 increased approximately two-fold from 3 to 15 months then remained high thereafter (152). Among other related genes, the expression of Fxr and Hnf-4 remained relatively stable with age in both male and female mice (152). Shp in the liver was relatively stable with age in male mice, whereas it decreased from 12 to 15 months and remained low thereafter in female mice (152). The expression of Fgf15 in the ileum remained stable in male mice from 6 to 27 months, while in female mice it peaked at 12 months and decreased thereafter (152). A study of aging and bile acid synthesis was performed on human surgical liver biopsy samples. Aging was inversely correlated with bile acid synthesis activity as well as the mRNA expression of CYP7A1 (156).

1.7 Hypothesis and Objectives of the Study

1.7.1 Hypothesis

Bile acid homeostasis is largely maintained by bile acid synthesis and enterohepatic circulation. The aforementioned studies suggest that age-related changes in processes involved in bile acid enterohepatic circulation and bile acid synthesis exist. However, the evidence is limited. The rationale for our studies and the basis for our hypothesis (see below) come from two human studies (153, 154). Salemans et al. (153) examined fasting and postprandial serum

levels of bile acids in 12 older (mean of 67 years of age) and 12 younger (mean of 37 years of age) subjects. They found that the postprandial serum level of conjugated bile acids is significantly lower in the older subjects compared to younger subjects. Specifically, the postprandial serum level of conjugated cholic acid was 39% lower in older subjects, and chenodeoxycholic acid was 24% lower (153). The other study, by Nagengast et al. (154) examined fecal bile acid profiles in healthy subjects of three different age groups (mean ages of 22, 48 and 67 years). They observed an increase in the fecal concentration of secondary bile acids in the older adults compared to the younger adults (154). Together, these data may suggest that intestinal bile acid absorption is reduced in older individuals. This led to our hypothesis that there is a reduction in intestinal bile acid absorption and the expression of bile acid transporters with increasing age. Although the human studies mentioned above suggest that bile acid absorption decreases with aging, this has never been actually measured. Also, no study has examined the influence of frailty on intestinal bile acid absorption or the transporters involved in enterohepatic circulation, and this was also examined for my thesis project.

1.7.2 Objectives

The purpose of the study was to examine the influence of both age and frailty level on intestinal bile acid absorption and the transporters involved in bile acid enterohepatic circulation. The two objectives were to measure 1) the rate of bile acid transport across the mouse terminal ileum and 2) the mRNA expression level of intestinal and hepatic bile acid transporters, Fxr, Fgf15, and Cyp7a1 as a function of age and frailty level. C57BL/6 mice of varying ages and frailty levels were used in our studies. For objective 1 we measured the rate of taurocholate transport across the freshly dissected mouse terminal ileum in Ussing chambers. For objective 2

we used qPCR to measure the expression level of Asbt, Ostα/β, Fxr and Fgf15 in the ileum, as well as Ntcp, Bsep, Oatp1b2, Fxr and Cyp7a1 in the liver.

TABLE 1.1

Chemical structure of bile acids and their conjugates

Bile acid	**Conjugated forms**	
Cholic acid	Glycocholate	Taurocholate
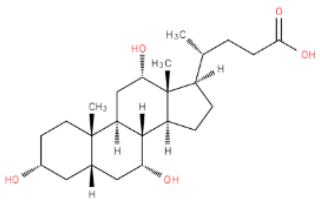	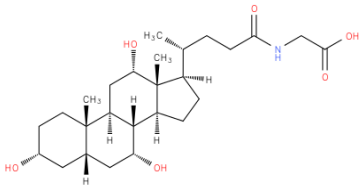	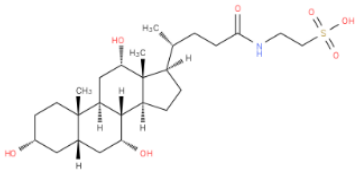
Chenodeoxycholic acid	Glycochenodeoxycholate	Taurochenodeoxycholate
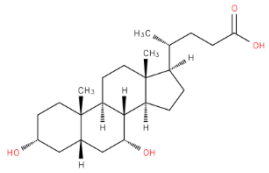	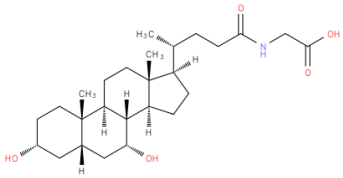	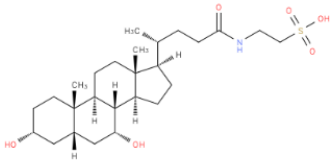
Deoxycholic acid	Glycodeoxycholate	Taurodeoxycholate
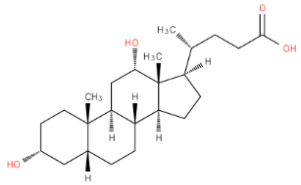	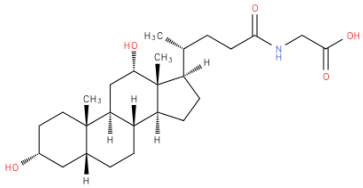	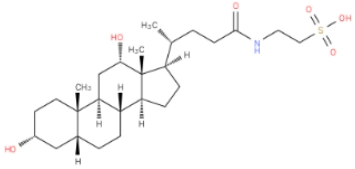
Lithocholic acid	Glycolithocholate	Taurolithocholate
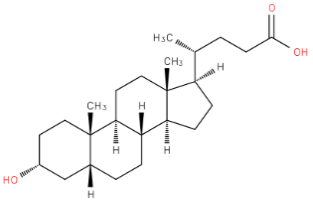	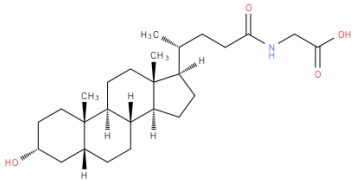	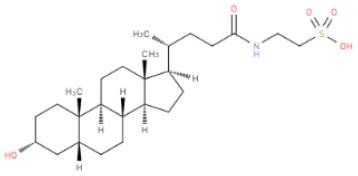

Images of the chemical structures are from Chemical Entities of Biological Interest (ChEBI)

(http://www.ebi.ac.uk/chebi/init.do)

Figure 1.1

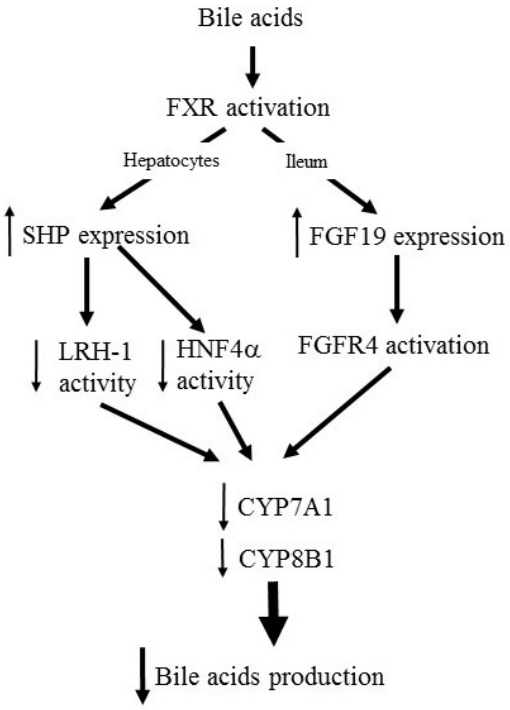

Figure 1.1. A simplified schematic of the two major pathways by which bile acids regulate their own synthesis. In the FXR/SHP pathway, FXR in hepatocytes is activated by bile acids. This activation results in increased transcription of an inhibitory nuclear factor, SHP. SHP subsequently represses the transcription of LRH-1 and HNF4α, leading to suppression of CYP7A1 and CYP8B1 transcription. In the FXR/FGF19/FGFR4 pathway, FXR in epithelial cells of the ileum is activated by bile acids. FXR activation leads to the production of FGF19, which then travels to hepatocytes via the portal vein system. FGF19 binds to FGFR4 on the hepatocyte membrane and the subsequent signal transduction mechanism leads to a suppression of CYP7A1 and CYP8B1 transcription.

Figure 1.2

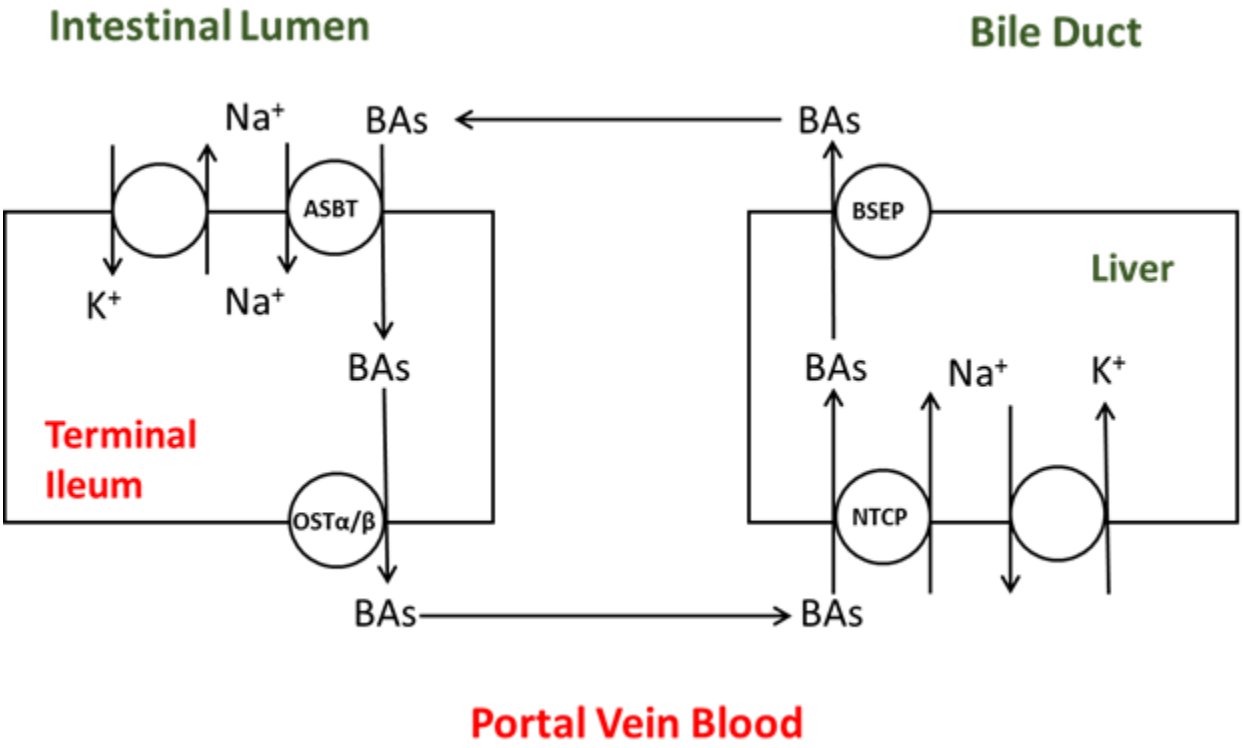

Figure 1.2. Shown are the major transporters involved in the enterohepatic circulation of bile acids. In the terminal ileum, bile acids (BAs) are taken up into epithelial cells by the apical sodium-dependent bile acid transporter (ASBT). Bile acids subsequently enter the portal vein circulation by facilitated diffusion through the organic solute transporter α and β dimer (OSTα/β). Upon reaching the liver, bile acids are taken up into the hepatocytes by the Na^+-taurocholate cotransporting polypeptide (NTCP). Bile acids in the hepatocytes are secreted into the bile canaliculi by the ATP-dependent bile salt export pump (BSEP).

Figure 1.3

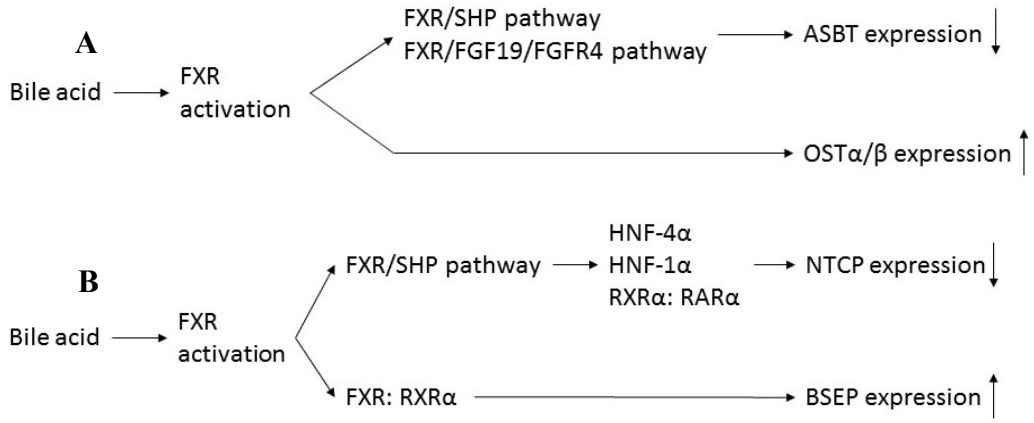

Figure1.3. Dominant pathways for bile acid transporter regulation by bile acids. **Figure 1.3A** shows the regulation of intestinal bile acid transporters by bile acids. Upon activation by bile acids, FXR activates both FXR/SHP and FXR/FGF15/FGFR4 pathways, leading to decreased ASBT expression. Activated FXR also increases transcription of OSTα/β. **Figure 1.3B** shows the regulation of liver bile acid transporters by bile acids. Upon activation by bile acids, FXR induces the expression of SHP, which acts on different downstream nuclear factors in different species, to downregulate NTCP expression. FXR activation also leads to the formation of the FXR: RXRα heterodimer, which directly stimulates the expression of BSEP.

Figure 1.4

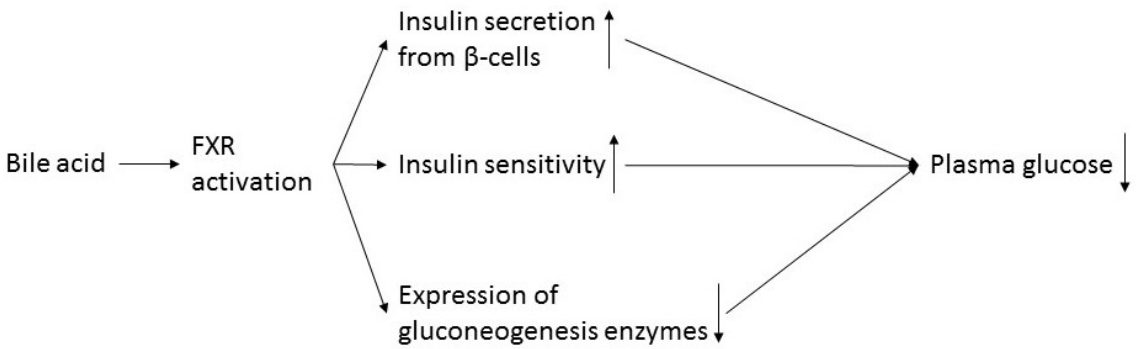

Figure 1.4. The effect of bile acids acting through FXR on glucose homeostasis. Following activation by bile acids, FXR induces insulin secretion from pancreatic β-cells. The activation of FXR also leads to improved peripheral insulin sensitivity and reduced activity of enzymes required for hepatic gluconeogenesis. These effects lead to the lowering of plasma glucose and improvement of diabetes in mouse models.

Figure 1.5

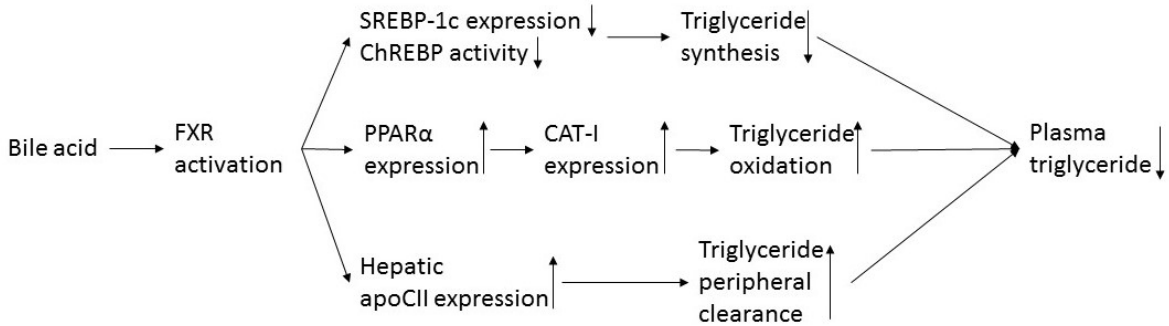

Figure 1.5. The effect of bile acids acting through FXR on triglyceride homeostasis. Upon activation by bile acids, FXR reduces the expression of SREBP-1c and the activity of ChREBP, which leads to downregulation of lipogenic genes and decreased triglyceride synthesis. FXR also stimulates the production of PPARα, resulting in an increased expression of the major enzyme in fatty acid β-oxidation, CAT-I, and subsequently elevated triglyceride oxidation. FXR also increases the hepatic production of apoCII, which stimulates the activity of lipoprotein lipase in endothelial cells. Increased lipoprotein lipase activity stimulates the peripheral clearance of triglycerides. Together, all of these effects lower the plasma level of triglycerides.

CHAPTER 2: MATERIALS AND METHODS

2.1 Experimental Animals

Male C57BL/6 mice, ranging from 89-953 days old, were used in these studies. The mice were housed in the Carleton Animal Care Facility at Dalhousie University, and we obtained the mice from Dr. Susan Howlett's laboratory at Dalhousie University. The mice were kept under a 12-hour light/dark cycle and were allowed free access to food and water. The animals were fed a standard diet (ProLab RMH 3500, LabDiet). All experiments adhered to the Canadian Council on Animal Care Guide to the Care and Use of Experimental Animals (Canadian Council on Animal Care, Ottawa, ON: Vol. 1, 2nd edition 1993:1), and all protocols were approved by the Dalhousie University Committee on Laboratory Animals.

2.2 Frailty Assessment

A non-invasive frailty assessment was used to quantify the degree of frailty of the mice used in these experiments (148). The non-invasive frailty assessment combines 31 readily observed, published signs of deterioration in aging mice, focusing on the integumentary, musculoskeletal, vestibulocochlear, ocular, digestive, genitourinary and respiratory systems, and signs of discomfort, body temperature and weight (148), see **Table 2.1** for the details of the non-invasive mouse frailty assessment form. Each variable receives a value of 0 (no deficit), 0.5 (mild deficit) or 1 (severe deficit). Data for the 31 potential deficits are summed and divided by the total number of variables to yield a frailty index score between 0 (no deficits) and 1 (all possible deficits) for each animal. When human frailty index scores were calculated from the Survey of Health, Aging and Retirement in Europe (SHARE) human database, the exponential relationship between frailty index scores and age was virtually identical in mice and humans

when age was normalized by the 90% mortality of each group (148). This indicates that rates of deficit accumulation with time are similar in mice and humans. Also, the highest frailty index scores in mice approach the submaximal limit to frailty reported in humans (148, 157). These data demonstrate that the frailty index developed for use in aging animals exhibits key features of the frailty index established for use clinically. The frailty assessment shows high reproducibility from trial to trial and shows high reliability between different frailty assessment raters (157). The person performing the frailty assessment and the person performing the experiments were different. The frailty index score was not revealed to the person performing the experiments, until after they were completed.

2.3 Chemical Reagents

The [^{3}H]-taurocholic acid (ART1368) with a specific activity of 10 mCi/mmol was from American Radiolabeled Chemicals, Inc. (St. Louis, MO, USA). TaqMan qPCR probes and TaqMan Universal Master Mix II with UNG were from ThermoFisher Scientific. RNAlater, RNeasy Mini kit, and the QuantiTect Reverse Transcription kit were from Qiagen. The Experion RNA StdSens Analysis kit was from Bio-Rad. All other chemicals and reagents were from Sigma-Aldrich or ThermoFisher Scientific.

2.4 Bile Acid Transport Measurement on Mouse Ileum Tissue

2.4.1 Tissue dissection and processing

Animals underwent two different euthanasia procedures before tissue dissection, and the euthanasia was performed immediately after calculating the frailty index of the mouse. The first group of animals' euthanasia procedure involved the intraperitoneal injection of pentobarbital sodium 200mg/kg with heparin 3000U/kg. The heart was then removed surgically for other purposes (158). The second group of animals were subject to a technique called intracardiac

programmed electrical stimulation prior to euthanasia. Briefly, mice were anesthetized using 2% isoflurane inhalation and a 1.1F electrophysiology catheter was placed into the right heart via the jugular vein. This allows the measurement of various cardiac electrophysiological parameters. During this time, surface ECGs were continuously recorded by 30 gauge subdermal electrodes and body temperature was maintained at 37°C. Following baseline measurements of several cardiac electrophysiological parameters, carbachol (0.1mg/kg, IP injection) was administered and the measurements were repeated. Animals were typically injected with carbachol 45 minutes after the start of experiments and experiments were completed within 75 minutes. There were no signs of hemodynamic instability throughout the experiment. Following experimentation, blood samples were taken by cardiac puncture, animals were sacrificed by cervical desolation, and the hearts were removed (159). Animals underwent the first euthanasia procedure accounted for approximately 60% of all the animals while animals underwent the second accounted for the rest.

Approximately 10 minutes after euthanasia, the animals were prepared for dissection of the terminal ileum and liver under a stereomicroscope (Olympus SZ51). The entire dissection procedure took ~20 minutes. The ileum was located using the cecum as a guide. Using surgical scissors, the ileum was first cut at the point where it enters the cecum, and the second cut was made ~1.5 cm above the cecum. The segment of ileum was placed in a Petri dish containing room temperature phosphate buffered saline (PBS) and the adventitia was carefully removed with iris scissors. The segment of ileum was then cut with a scalpel into three equivalent size pieces (~0.5 cm long). The two pieces closest to the cecum were used for taurocholate transport measurement in Ussing chambers, and the piece most distal to the cecum for RNA analysis. For transport measurement, the tissue was placed over the aperture of one semi-chamber (i.e. half of

a chamber) of an Ussing chamber and the lumen was exposed by making a sagittal cut with iris scissors. The intestinal content was carefully removed using forceps and the tissue was stretched over the aperture. The two semi-chambers were then put together thus sealing the tissue between the aperture of the Ussing chamber. The tissue was rinsed once with Kreb's solution to remove any remaining intestinal content. For consistency, the tissue closest to the cecum was used for the measurement of the unidirectional lumen-to-blood flux (absorption) and the other for the measurement of the unidirectional blood-to-lumen flux (secretion) of taurocholate. The lumen of the third tissue was also exposed, the intestinal content removed, and it was placed in > 10 volumes of RNAlater. For the liver, a small segment of the median lobe was removed and placed in ~10 volumes of RNAlater. The tissues in RNAlater were stored at -80°C until processing for gene expression analysis.

2.4.2 Ussing chambers and apparatus

The ileum tissue was mounted in Ussing chambers with an aperture size of 0.126 cm^2 (**Figure 2.1A**). Each semi-chamber contained 1.2 ml of Kreb's buffer (containing in mM: 117 NaCl, 4.5 KCl, 20 $NaHCO_3$, 6 D-glucose, 1.5 $CaCl_2$, 1 $MgCl_2$ and 10 hydroxyethyl piperazineethanesulfonic acid, HEPES; pH=7.4). The Ussing chambers were placed in an apparatus designed to continuously stir the buffer inside the chambers, and to maintain the buffer temperature at 37°C and pH at 7.4. **Figure 2.1B** shows the Ussing chamber apparatus. When placed in the apparatus, the Ussing chambers sat on top of a metal plate, below which was circulating water connected to a circulating water bath that was heated to 42°C in order to maintain the internal buffer temperature at 37°C. Humidified medical grade 95% O_2/5% CO_2 was continuously blown on top of the buffer in each semi-chamber to maintain pH at 7.4. The

small stir bars inside each semi-chamber were driven by external stir plates lying below the Ussing chamber apparatus.

2.4.3 Electrophysiology

After being placed in the Ussing chambers and apparatus, the tissues were given ~10 minutes to recover prior to recording transepithelial electrical properties and beginning transport measurement. Ag-AgCl electrodes were used as short-circuiting electrodes (i.e., voltage-clamping) and to measure transepithelial electrical properties of the ileum. The transepithelial electrical properties measured included the transepithelial potential difference (TPD), short-circuit current (I_{sc}) and transepithelial resistance (TER). The electrodes were connected to the blood and lumen side of the ileum tissue using PE90 tubing containing solidified 3 mM KCl and 2% agar. The TPD and current (I) were monitored using a high impedance automatic dual voltage clamp (EVC 4000-4, World Precision Instructions, Sarasota, FL, USA) interfaced with a PowerLab 28T and LabChart software (ADInstruments, Colorado Springs, CO, USA) for data collection. The TER was determined according to Ohm's Law ($TER = \Delta TPD/I$) from the change in TPD following a brief 10 μA current passed through the tissue using the voltage clamp. We determined transepithelial electrical properties at the beginning and end of each experiment in order to monitor tissue viability. At the end of the experiment, after taking the final TPD and I recordings, the epithelium was punctured and recordings were taken again to account for voltage drift in the electrodes during the course of the experiment and for the amount of fluid resistance between the electrodes. Electrophysiological recordings took ~2 minutes. Tissues that had a resistance lower than 40 $\Omega \cdot cm^2$ at the end of the experiment, or where transport did not achieve steady-state, were excluded from data analysis. A low tissue resistance indicates a non-viable tissue.

2.4.4 Measurement of transepithelial taurocholate transport

Transport experiments were initiated immediately after the electrophysiological measurements. As previously stated, we required 2 pieces of ileum from each mouse for the transport experiment. One piece was needed to determine the unidirectional blood-to-lumen flux of taurocholate (secretion) and the other for the unidirectional lumen-to-blood flux of taurocholate (absorption). All transport experiments were performed under voltage-clamped conditions to eliminate the electrochemical gradients across the ileum tissue. Bile acid absorption is mainly mediated by intestinal bile acid transporters. Bile acid secretion is minimal compared to absorption and is likely the result passive diffusion. The net transepithelial taurocholate transport, which is the difference between absorption and secretion, represents the active, transporter-mediated bile acid transport. **Figure 2.1C** demonstrates the measurement of unidirectional fluxes of taurocholate across the ileum tissue. 5 μM taurocholate (non-radiolabeled) was added to the Kreb's solution bathing both sides of the tissue, and approximately 0.1-0.2 μM ^{3}H-taurocholate was added to either the lumen or blood side of the tissue. To determine the unidirectional blood-to-lumen flux, the ^{3}H-taurocholate was added to the blood side only. To determine the unidirectional lumen-to-blood flux, the ^{3}H-taurocholate was added to the lumen side only. The side receiving ^{3}H-taurocholate at the beginning of the experiment was termed the 'hot side' and the other the 'cold side'. Duplicate 50 μL samples were collected every 30 minutes from the cold side and replaced with an equal volume of Kreb's buffer containing 5 μM unlabelled taurocholate. Duplicate 10 μL samples were collected from the hot side at the beginning and end of the experiment to determine the concentration of ^{3}H-taurocholate on the hot side at the beginning and end of each experiment. The amount of ^{3}H-

taurocholate was determined by liquid scintillation spectrometry (LS6500, Beckman Coulter, CA, USA or Tri-Carb 2910TR, PerkinElmer, MA, USA).

2.5 RNA Isolation, cDNA Synthesis, and Quantitative Polymerase Chain Reaction

Samples of ileum and liver stored at -80°C in RNAlater were thawed on ice prior to RNA extraction. Approximately 30 mg of tissue was homogenized using a Qiagen TissueRuptor and RNA was subsequently extracted using the Qiagen RNeasy Mini Kit according to the manufacturer's instructions. RNA concentration and purity (260/280 ratio) was determined with a Cytation 3 Imaging System (BioTek, VT, USA). RNA integrity of the samples was determined with an Experion RNA StdSens Analysis Kit and an Experion Automated Electrophoresis System (Bio-Rad, Mississauga, ON), according to the manufacturer's instructions. RNA quality indicator (RQI) is a parameter that assesses the integrity of RNA samples used in Experion Automated Electrophoresis System. All samples had RQI values greater than 8.0, and were used for cDNA synthesis. The cDNA synthesis was performed with the Qiagen QuantiTect Reverse Transcription Kit, according to the manufacturer's instructions. 0.5 µg of RNA was used in each cDNA synthesis reaction, yielding a final volume of 40 µL.

The qPCR reactions were assembled using 2 µL of cDNA, 5 µL of TaqMan Universal Master Mix II with UNG, 2.5 µL of nuclease-free water and 0.5 µL of TaqMan Gene Expression Assay directed against the gene of interest or a housekeeping gene. For each sample, qPCR was run in duplicate. Negative controls included water in the reaction, instead of cDNA. **Table 2.2** shows the TaqMan Gene Expression Assays used in these studies. The assays contained a TaqMan probe with a FAM™ dye label for quantification of cDNA amplification. The qPCR

was performed with a Bio-Rad CFX Connect Real-Time PCR Detection System using the following conditions:

1) 50°C for 2 minutes
2) 95°C for 10 minutes
3) 95°C for 15 seconds then 60°C for 1 minute, repeated 39 times
4) 65°C for 5 seconds
5) 95°C for 30 seconds

The $\Delta\Delta C_T$ method was used for relative quantification of mRNA expression where mRNA expression from an animal of 223 days old with a frailty index of 0.1048 was set to 1. In addition to the gene of interest, the $\Delta\Delta C_T$ method requires that the expression of a housekeeping gene be examined. In order for the $\Delta\Delta C_T$ method to be accurate for relative mRNA quantification, it is required that the PCR amplification efficiency of the gene of interest and the housekeeping gene are similar. To find the appropriate housekeeping gene, we examined the amplification of 3 different housekeeping genes (Eif2b1, Polr2a, and β2-microglobin) alongside the amplification of each gene of interest. Specifically, cDNA was serially diluted over a 250-fold range (1, 0.5, 0.1, 0.02 and 0.004), and qPCR was performed on each gene of and each housekeeping gene. The difference in Threshold Cycle (C_T) value between the gene of interest and the housekeeping gene was calculated at each cDNA dilution. This difference was then plotted against the Log10 of cDNA concentration, and a linear regression was performed. A housekeeping gene is considered appropriate for use in relative mRNA quantification when the observed linear regression slope is between -0.1 and 0.1. **Figure 2.2** shows an example of amplification efficiency experiments between Oapt1b2 and β2-microglobin, and Oatp1b2 and Eif2b1. These two examples were chosen since one housekeeping gene is appropriate for use in

relative mRNA quantification (Oapt1b2 with β2-microglobin) whereas the other is inappropriate (Oatp1b2 with Eif2b1). Using this method, we found appropriate housekeeping genes for each gene of interest, except for Ostα, for which the closest housekeeping gene had a slope of 0.133 ± 0.045. However, since the slope approximated 0.1, that housekeeping gene was used in the relative quantification of Ostα mRNA expression. **Table 2.3** shows the housekeeping gene used for Relative mRNA quantification for each gene of interest. All C_T values were in the range of 15 to 26.

2.6 Data Analysis

Linear regression analysis and unpaired two-tailed *t*-tests were performed with GraphPad Prism (version 6). Multiple linear regression analysis and partial correlation analysis were performed with SPSS (version 23). For regression analysis, the Pearson correlation coefficient was used to describe the goodness-of-fit between dependent and independent variables. Data are reported as mean ± standard error of the mean. Statistical significance was set at the $p<0.05$ level.

Table 2.1

Table 2.1. Mouse Frailty Assessment Form

Date: _____

Mouse #: _____ **Date of Birth:** _____ **Sex:** F M

Body weight (g): _____ **Body surface temperature (°C):** _____

Rating: 0 = absent 0.5 = mild 1 = severe

				NOTES:
➢ **Integument:**				
❖ Alopecia	**0**	**0.5**	**1**	_____
❖ Loss of fur colour	**0**	**0.5**	**1**	_____
❖ Dermatitis	**0**	**0.5**	**1**	_____
❖ Loss of whiskers	**0**	**0.5**	**1**	_____
❖ Coat condition	**0**	**0.5**	**1**	_____
➢ **Physical/Musculoskeletal:**				
❖ Tumours	**0**	**0.5**	**1**	_____
❖ Distended abdomen	**0**	**0.5**	**1**	_____
❖ Kyphosis	**0**	**0.5**	**1**	_____
❖ Tail stiffening	**0**	**0.5**	**1**	_____
❖ Gait disorders	**0**	**0.5**	**1**	_____
❖ Tremor	**0**	**0.5**	**1**	_____
❖ Forelimb grip strength	**0**	**0.5**	**1**	_____
❖ Body condition score	**0**	**0.5**	**1**	_____
➢ **Vestibulocochlear/Auditory:**				
❖ Vestibular disturbance	**0**	**0.5**	**1**	_____
❖ Hearing loss	**0**	**0.5**	**1**	_____
➢ **Ocular/Nasal:**				
❖ Cataracts	**0**	**0.5**	**1**	_____
❖ Corneal opacity	**0**	**0.5**	**1**	_____
❖ Eye discharge/swelling	**0**	**0.5**	**1**	_____
❖ Microphthalmia	**0**	**0.5**	**1**	_____
❖ Vision loss	**0**	**0.5**	**1**	_____
❖ Menace reflex	**0**	**0.5**	**1**	_____
❖ Nasal discharge	**0**	**0.5**	**1**	_____
➢ **Digestive/Urogenital:**				
❖ Malocclusions	**0**	**0.5**	**1**	_____
❖ Rectal prolapse	**0**	**0.5**	**1**	_____
❖ Vaginal/uterine/penile prolapse	**0**	**0.5**	**1**	_____
❖ Diarrhoea	**0**	**0.5**	**1**	_____
➢ **Respiratory system:**				
❖ Breathing rate/depth	**0**	**0.5**	**1**	_____
➢ **Discomfort:**				
❖ Mouse Grimace Scale	**0**	**0.5**	**1**	_____
❖ Piloerection	**0**	**0.5**	**1**	_____
❖ **Temperature score:** _____				
❖ **Body weight score:** _____				

Total Score/ Max Score:

TABLE 2.2

Table 2.2. TaqMan gene expression assays used for qPCR

Gene	Assay
Asbt (Slc10a2)	Mm00488258_m1
Ostα (Slc51a)	Mm00521530_m1
Ostβ (Slc51b)	Mm01175040_m1
Fxr (Nr1h4)	Mm00436425_m1
Ntcp (Slc10a1)	Mm00441421_m1
Bsep (Abcb11)	Mm00445168_m1
Oatp1b2 (Slco1b2)	Mm00451510_m1
Cyp7a1	Mm00484150_m1
β2-microglobin	Mm00437762_m1
Polymerase (RNA) II (DNA directed) polypeptide A (Polr2a)	Mm00839502_m1
Eukaryotic translation initiation factor 2B, subunit α (Eif2b1)	Mm00460997_m1

TABLE 2.3

Table 2.3. Housekeeping genes selected for relative quantification of mRNA for bile acid transporters, Fxr, Fgf15, and Cyp7a1

Gene of interest	Housekeeping gene	Slope
Asbt	β2m	0.059 ± 0.028
Ostα	β2m	0.133 ± 0.045*
Ostβ	β2m	-0.097 ± 0.065
Fxr (ileum)	β2m	0.005 ± 0.026
Fgf15	β2m	-0.065 ± 0.035
Ntcp	β2m	-0.011 ± 0.044
Bsep	β2m	-0.096 ± 0.018
Fxr (liver)	β2m	-0.043 ± 0.097
Cyp7a1	Polr2a	0.066 ± 0.034
Oatp1b2	β2m	-0.009 ± 0.073

*, the slope is above the threshold level of 0.1, however β2m is still used for the relative quantification of Ostα since this slope is the closest to 0.1 among all housekeeping genes and the slope approximates 0.1.

Figure 2.1

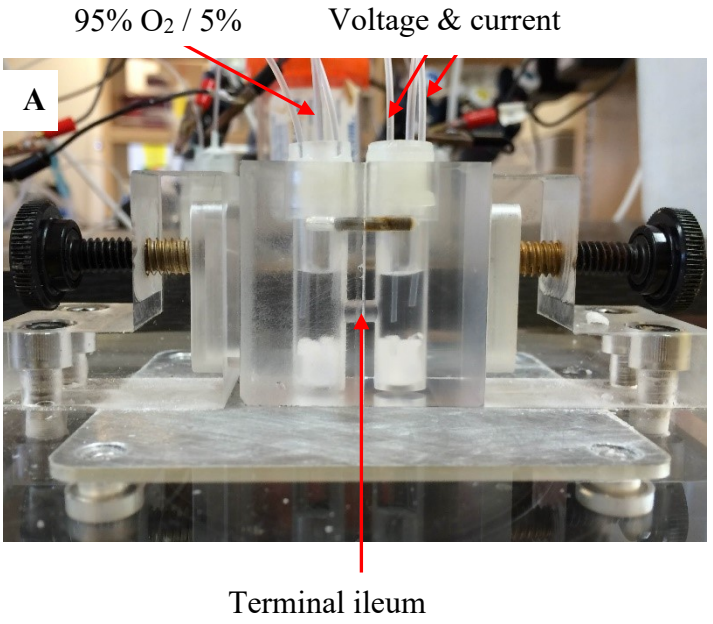

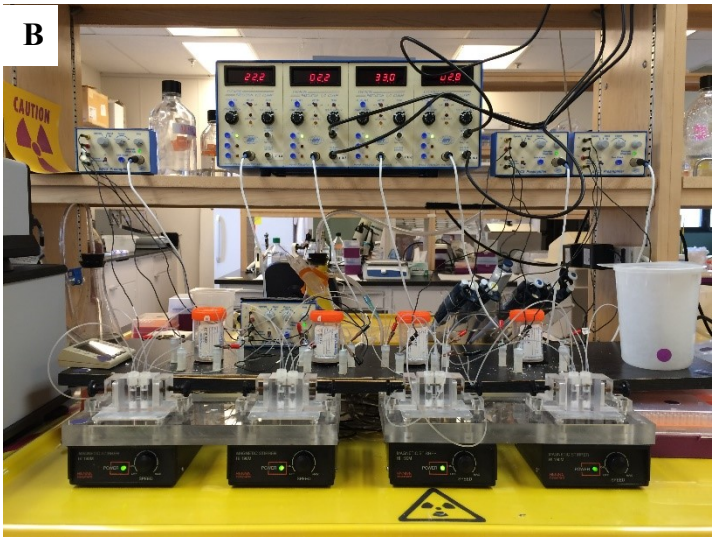

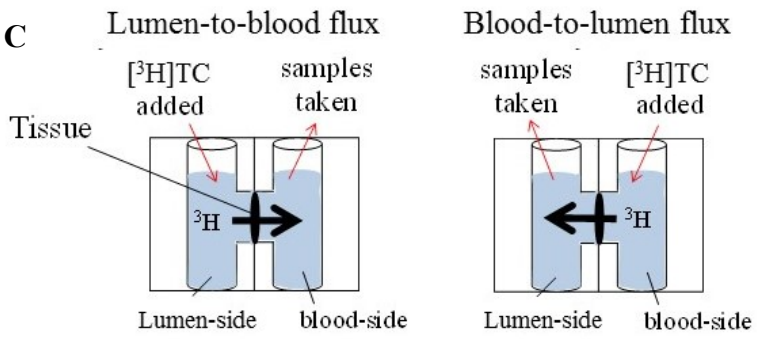

Figure 2.1. Ussing chamber. **Figure 2.1A** shows an individual Ussing chamber. The tissue is placed over the aperture between two semi-chambers. Moisturized CO_2 is delivered to each semi-chamber to maintain the pH of the buffer during the experiment. Electrophysiology parameters are measured by electrodes inserted into the buffer. **Figure 2.1B** shows the entire system, including four separate Ussing chambers. **Figure 2.1C** demonstrates how the absorptive and secretory bile acid fluxes are measured. The difference between the two fluxes stands for the net absorption of bile acid by terminal ileum.

FIGURE 2.2

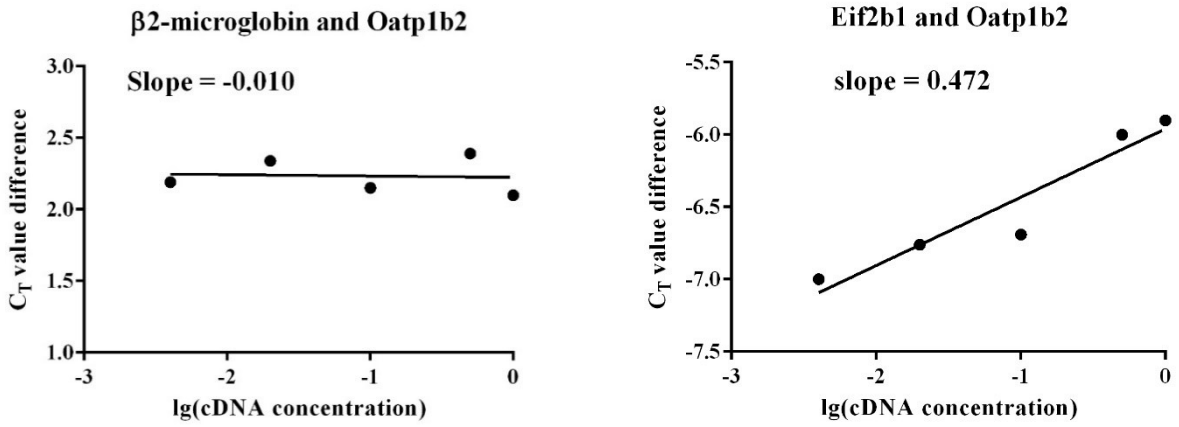

Figure 2.2. Shown are examples of amplification efficiency data used for selecting an appropriate housekeeping gene for determination of relative mRNA expression of bile acid transporters, Fxr, Fgf15, and Cyp7a1 by the $\Delta\Delta C_T$ method – the example shown is for Oatp1b2. The qPCR was performed on serially diluted mouse liver cDNA. The difference between C_T values of the housekeeping gene and Oatp1b2 was plotted against the Log_{10} of the cDNA concentration. Linear regression analysis was then performed. The left panel figure shows an amplification efficiency plot between Oatp1b2 and β2-microglobin – the linear regression slope is -0.010. The right panel figure shows an amplification efficiency plot between Oatp1b2 and Eif2b1 – the linear regression slope is 0.472. A housekeeping gene yielding an amplification efficiency plot with a slope between -0.1 and 0.1 is considered appropriate for use in relative mRNA quantification by the $\Delta\Delta C_T$ method. Thus, β2m was used in the analysis of Oatp1b2 mRNA expression in mouse liver. Amplification efficiency experiments were run between each gene of interest and each housekeeping gene (β2m, Eif2b1, and Polr2a) in order to find the appropriate housekeeping gene (see Table 2.2 for the housekeeping genes used for mRNA quantification of each gene of interest).

CHAPTER 3: RESULTS

3.1 Relationship between Frailty Index and Age in Male C57BL/6 Mice

The animals used were between 89-953 days old (~3 months to 31 months of age), and they all underwent frailty index scoring prior to experiments. Using an online mouse-to-human age converter (http://www.age-converter.com/mouse-age-calculator.html/), this would translate into ~20-100 years old in human years. For each animal, their age was plotted against their frailty index score in order to examine the relationship between age and frailty level (**Figure 3.1**). A significant positive linear correlation between age and frailty index score was observed (R^2=0.718, p<0.0001, n=21, **Figure 3.1A**). A previous study had shown that as male C57BL/6 mice become older, there is an exponential increase in their frailty level (148). Accordingly, we performed non-linear regression using an exponential function and observed a similar significant relationship between age and frailty index score (R^2=0.740, p<0.0001, n=21, **Figure 3.1B**). We did observe variation in frailty level in animals of the approximate same chronological age. For example, for animals of ~600 days of age (~20 months), their frailty index score ranged ~3-fold. It is apparent from these data that as animals become older they become increasingly frail. Further studies were designed to examine the effect of age and frailty level on taurocholate transport by the ileum in Ussing chambers and on the mRNA expression of intestinal and hepatic genes related to bile acid enterohepatic circulation. See **Table 3.1** for the individual age and frailty index data of the experimental mice.

3.2 Transepithelial Electrical Properties of the Mouse Ileum

Transepithelial electrical properties across the mouse ileum in Ussing chambers were determined prior to and after intestinal taurocholate transport experiments. This was done to

assess tissue health, and to determine if the tissues remained viable throughout the time course of the experiments (2-3 hours). The transepithelial electrical properties measured were the transepithelial resistance (TER), the transepithelial potential difference (TPD) and short-circuit current (I_{sc}). The I_{sc} is the current required to negate the TPD generated by the tissue *ex vivo*. In this experimental preparation, the TPD is a function of active salt and glucose transport by the tissue. The TER is a measure of the tight junctional resistance across the intestinal paracellular pathway. If the epithelium dies or leaks, then the TER, TPD, and I_{sc} approximate zero. **Table 3.2** shows the average starting and ending transepithelial electrical properties across the mouse ileum in our studies using Ussing chambers. There was a significant negative linear correlation between starting TER and frailty index score (R^2=0.242, p=0.045, n=17, **Figure 3.2A**). In contrast, there was no apparent correlation between age and TER (**Figure 3.2B**). The TPD and I_{sc} showed no relationship with age or frailty index score (data not shown).

3.3 Representative Taurocholate Transport Experiments

Representative experiments showing transepithelial transport of taurocholate across the mouse ileum in Ussing chambers *ex vivo* are shown in **Figure 3.3**, with **Figure 3.3A** showing data from a younger mouse (209 days old, frailty index score 0.193) and **Figure 3.3B** showing data from an older mouse (613 days old, frailty index score 0.363). The transepithelial transport of taurocholate was measured under voltage-clamped conditions to eliminate the electrochemical gradients. So the net taurocholate flux was the result of active transport. In both cases, the secretory flux (blood-to-lumen flux, open squares and dashed line) is low and is likely the result of passive diffusion. In contrast, the absorptive flux (lumen-to-blood, open circles, dashed line) of taurocholate across the ileum is large – note, the symbols for net flux (closed squares, solid line) mask the symbols for the absorptive flux. In both **Figure 3.3A** and **Figure 3.3B**, the net

flux of taurocholate is in the direction of absorption and reached steady-state at ~2 hours. **Figure 3.3C** shows the unidirectional fluxes and net absorptive flux of taurocholate for tissues from the younger and older animal at the 3-hour time point, i.e., at steady-state. The younger less frail animal showed a greater capacity for active taurocholate absorption than the older frailer animal. The flux ratios (lumen-to-blood flux divided by the blood-to-lumen flux) were ~50 and 17 respectively (**Figure 3.3C**).

3.4 Intestinal Taurocholate Absorption and Its Correlation with Age and Frailty

Additional transport experiments were conducted using mice of varying ages and degrees of frailty, focusing on the rate of net taurocholate absorption at steady-state only (**Figure 3.4**). The net absorption rate of taurocholate at steady-state was plotted against each animal's age (**Figure 3.4A**) as well as their frailty index score (**Figure 3.4B**). There was considerable variability in the capacity for taurocholate absorption among the tissues examined, with an approximately 7-fold difference between the highest and lowest net transport rates. There was a significant negative linear correlation between taurocholate net absorption rate and age (R^2=0.383, p=0.006, n=18), and between taurocholate net absorption rate and frailty index score (R^2=0.328, p=0.013, n=18).

Since both age and frailty index showed significant linear correlation with the net absorption rate of taurocholate, we intended to perform multiple linear regression analysis and partial correlation analysis to determine the contribution of age and frailty to the observed change in taurocholate net absorption. With respect to the multiple linear regression analysis, it should be noted that multicollinearity exists between age and frailty, which violates an assumption. However, we still performed a multiple linear regression. The multiple linear

regression model showed a moderate significance (p=0.025) but does not provide a good fit for this dataset (adjusted R^2=0.306). However, neither age (p=0.25) nor frailty index score (p=0.75) is a significant factor in the multiple linear regression model. These findings suggest that multiple linear regression is not an appropriate model for this dataset. In terms of the partial correlation analysis, the dichotomous distribution of age violates an assumption that the independent variables are normally distributed. We still performed the partial correlation analysis to determine the relationship between taurocholate net absorption rate and age while controlling for frailty index score, and between taurocholate net absorption rate and frailty index score, while controlling for age. In the partial correlation analysis, there was no significant effect of age on taurocholate net absorption rate after controlling for frailty index score (p = 0.25). There was also no significant effect of frailty index score on taurocholate net absorption rate after controlling for age (p=0.75).

Since there was an obvious dichotomy in mouse age, we also analyzed the effect of age on taurocholate net absorption by performing an unpaired two-tailed *t*-test. In this analysis, we took the average taurocholate net absorption rate from animals younger than 200 days of age or less (4.62 ± 0.44 nmol · cm^{-2} · h^{-1}, n=9) and compared it to the average taurocholate net absorption rate from animals older than 600 days of age or more (2.24 ± 0.32 nmol · cm^{-2} · h^{-1}, n=8). The taurocholate net absorption rate is significantly lower in older animals (p=0.0006), 52% lower than the young animals, as shown in **Figure 3.4C**. The taurocholate net absorption rate from the mouse at ~400 days of age was omitted from the analysis. The average age of animals in the younger and older cohort were ~151 days (~6 months old) and ~752 days (~2 years old), respectively. These ages in the mouse would translate into ~34 and ~70 years of age in humans.

3.5 The mRNA Expression of Ileal Bile Acid Transporters as a Function of Ileal Taurocholate Net Absorption Rate

Since for most of the mice we had mRNA expression data in parallel with functional data from their ileum, we were interested to see if the mRNA expression of Asbt, Ostα, and/or Ostβ were predictive of the level of steady-state taurocholate absorption rate. **Figure 3.5** shows linear regression analysis of mRNA expression of the ileal transporters (Asbt and Ostα/β) as a function of taurocholate net absorption rate. Although there was a modest negative correlation between Asbt mRNA expression and taurocholate absorption rate, it was not statistically significant. There was also no significant correlation between Ostα or Ostβ mRNA expression and taurocholate absorption rate. These data indicate that mRNA expression of the pertinent bile acid transporters in the ileum are not predictive of taurocholate absorption rate.

3.6 The mRNA Expression of Bile Acid Transporters, Fxr, and Fgf15 in the Ileum as a Function of Age and Frailty

To examine the mechanistic basis for the decreased rate of intestinal bile acid absorption as a function of age and frailty, we examined the mRNA expression of the bile acid transporters Asbt, Ostα and Ostβ in the ileum by qPCR. We also examined the expression of Fxr and Fgf15 in the ileum. The expression of these gene showed no statistically significant correlation with either age or frailty index (**Figure 3.6**).

We also examined the expression level of Asbt, Ostα, Ostβ, Fgf15 and Fxr mRNA expression in the younger versus older cohort by *t*-test (**Figure 3.7**). The classification of young and old animals is the same as above mentioned cut-off value (i.e. 200 days old or less vs. 600 days old or more, for young group n=12, for old group n=9). The relative expression level of

Asbt was 45% significantly lower in the older cohort ($\Delta\Delta C_T$ values of 0.89 ± 0.14 vs. 0.47 ± 0.07, p=0.028, unpaired two-tailed *t*-test), whereas expression of Ostα, Ostβ and Fxr was not different between the two cohorts. These data indicate that at least at the extremes of age in the mice examined, there is a difference in expression of Asbt.

3.7 The mRNA Expression of Bile Acid transporters, Fxr, and Cyp7a1 in the Liver as a Function of Age and Frailty

Since hepatic bile acid transporters are necessary for enterohepatic bile acid circulation, their mRNA expression was examined, along with Fxr, and Cyp7a1. The transporters examined were Ntcp, Bsep, and Oatp1b2. **Figure 3.8** shows the expression of these genes as a function of age and frailty index score. Of the genes tested, only Ntcp (R^2=0.266, p=0.017) and Oatp1b2 (R^2=0.274, p=0.015) showed a significant negative correlation with age, but not with frailty index score. The expression of Bsep, Fxr, and Cyp7a1 showed no statistically significant correlation with either age or frailty index.

We also examined the expression level of Ntcp, Bsep, Oatp1b2, Fxr, and Cyp7a1 mRNA expression in the younger versus older cohort by *t*-test (**Figure 3.9**). The classification of young and old animals is the same as above mentioned cut-off value (i.e. 200 days old or less and 600 days old or more, for young group n=12, for old group n=7). The relative mRNA expression of Ntcp was 40% significantly lower ($\Delta\Delta C_T$ values of 1.004 ± 0.085 vs. 0.609 ± 0.119, p=0.0125, unpaired two-tailed *t*-test) and that of Oatp1b2 35% significantly lower ($\Delta\Delta C_T$ values of 0.915 ± 0.065 vs. 0.602 ± 0.108, p=0.0162, unpaired two-tailed *t*-test) in the older cohort – these two are also the genes that showed a negative correlation by linear regression analysis. The relative expression level of Bsep, Fxr and Cyp7a1 mRNA was not different between the younger and older cohorts.

Table 3.1

Table 3.1. Age and frailty index of individual mice

Mouse number	Age (days)	Frailty index
1	384	0.2016
2	903	0.3887
3	905	0.4355
4	923	0.4355
5	953	0.3548
6	207	0.2419
7	209	0.1935
8	210	0.2097
9	217	0.1532
10	224	0.1613
11	137	0.0645
12	613	0.3630
13	659	0.2180
14	628	0.2980
15	89	0.1770
16	90	0.1290
17	91	0.1130
18	666	0.2820
19	92	0.1290
20	671	0.2020
21	671	0.1770

TABLE 3.2

Table 3.2. Transepithelial electrical properties of the mouse ileum in Ussing chambers at the beginning and end of transport experiments

	Potential difference (mV)	Tissue resistance ($\Omega \cdot cm^2$)	Short-circuit current ($\mu A/cm^2$)
Beginning	1.89 ± 0.15	66.94 ± 4.06	-13.99 ± 1.59
Ending	1.63 ± 0.16	49.08 ± 5.04	-18.85 ± 3.10

Data are mean ± standard error of the mean of n=17 tissues.

FIGURE 3.1

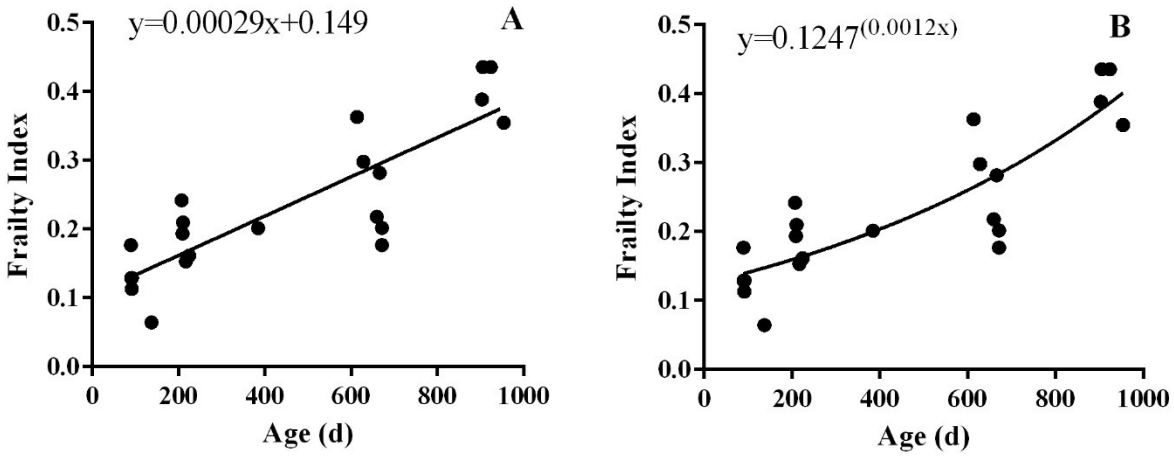

Figure 3.1. Shown are correlations between age and frailty index score in C57BL/6 mice as linear (A) and exponential (B) functions. The linear correlation between age and frailty index was significant (R^2=0.718, p<0.0001, n=21), as was the exponential correlation (R^2=0.741, p<0.0001, n=21). These data indicate that frailty index score increases steadily with age, with variation among animals of similar chronological age.

FIGURE 3.2

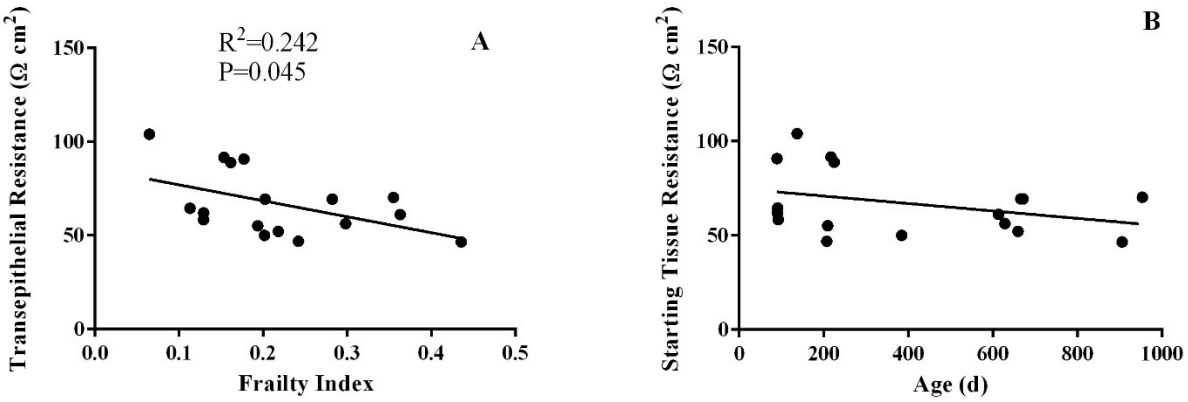

Figure 3.2. Shown is the starting transepithelial electrical resistance (TER) of the ileum from 17 different mice as a function of frailty index score (**Figure 3.2A**) and age (**Figure 3.2B**). There was a significant negative linear correlation between frailty index score and TER (R^2=0.242, p=0.045, n=17), but not between age and TER (R^2= 0.120, p=0.17, n=17). There was no correlation between the transepithelial electrical potential or short-circuit current as a function of frailty index score or age (data not shown).

FIGURE 3.3

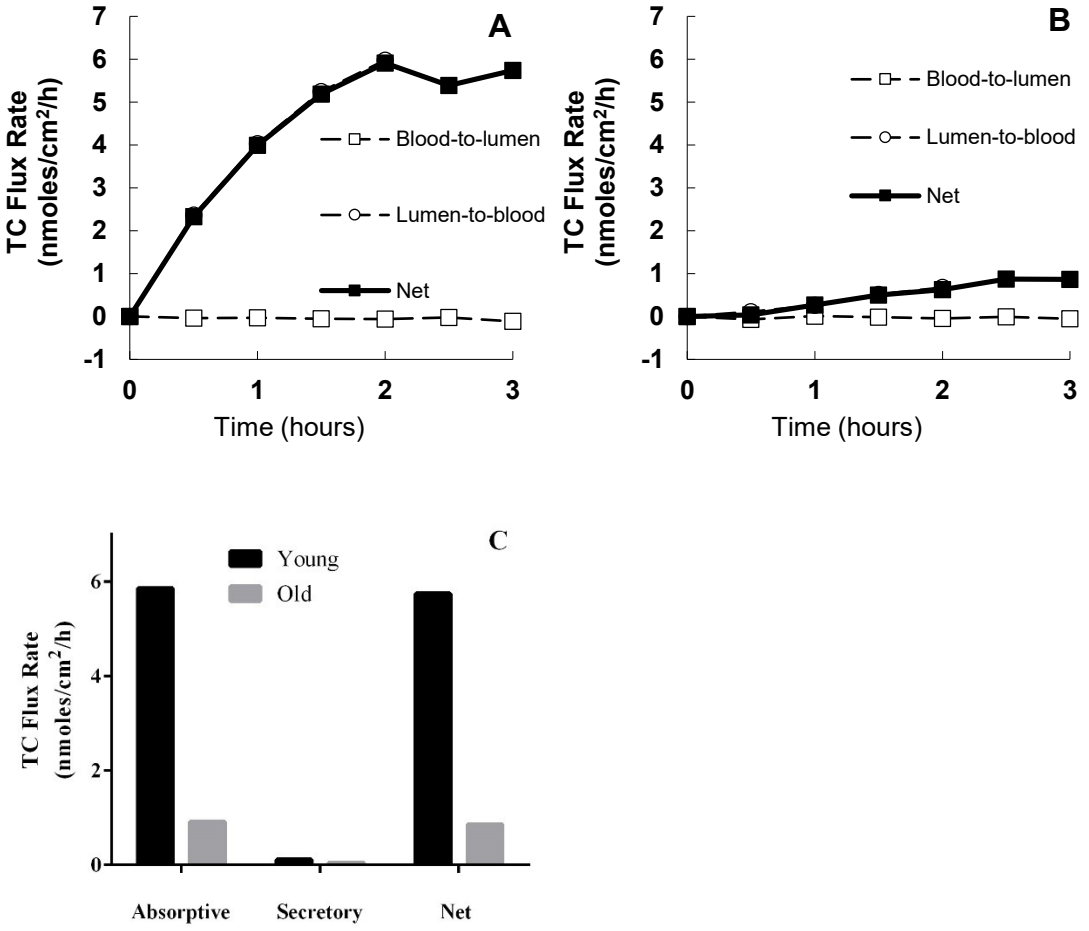

Figure 3.3. Shown are representative experiments examining the flux rate of taurocholate (TC) across the mouse ileum in Ussing chambers. **Figure 3.3A**) Taurocholate transport by ileum from a relatively young animal (209 days old, frailty score 0.19). **Figure 3.3B**) Taurocholate transport by ileum from a relatively old animal (613 days old, frailty score 0.36). Figures A and B show the unidirectional blood-to-lumen (secretory) and lumen-to-blood (absorptive) fluxes, and net active flux (the difference between the unidirectional fluxes) of taurocholate over a 3-hour period. Net active transport is in the direction of lumen-to-blood (absorption) and reaches steady-state at ~2 hours. **Figure 3.3C**) Unidirectional fluxes and net active flux of taurocholate by ileum from the young and old animal at a steady-state time point (3h). Note that net active absorption is greater in the younger less frail animal.

FIGURE 3.4

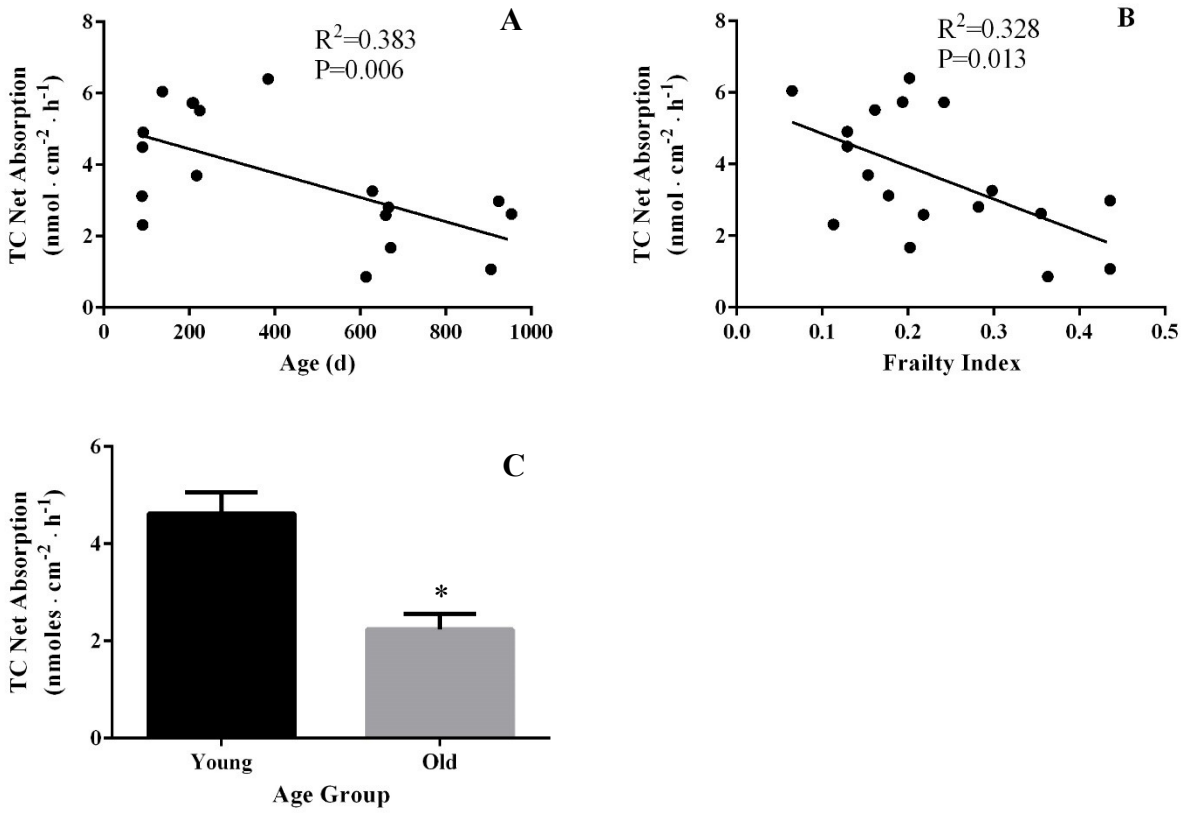

Figure 3.4. Shown are the effects of age and frailty index score on the net active absorption of taurocholate by the mouse ileum in Ussing chambers. Net active absorption of taurocholate by the ileum from 18 animals as a function of their age (**Figure 3.4A**) or frailty index score (**Figure 3.4B**). There was a significant negative linear correlation between net active taurocholate absorption with age (R^2=0.383, p=0.006, n=18), as well as frailty index score (R^2=0.328, p=0.013, n=18). **Figure 3.4C** showed that mice older than approximately 600 days of age (752 days old on average, n=8) had a significantly lower net active taurocholate absorption rate compared to mice of approximately 200 days old or younger (151 days old on average, n=9) – 2.24 ± 0.32 nmol · cm^{-2} · h^{-1} vs 4.62 ± 0.44 nmol · cm^{-2} · h^{-1}, p=0.0006, two-tailed *t*-test). Data are expressed as mean ± standard error of the mean. (*, significantly different from young mice, p<0.05, two-tailed unpaired *t*-test)

FIGURE 3.5

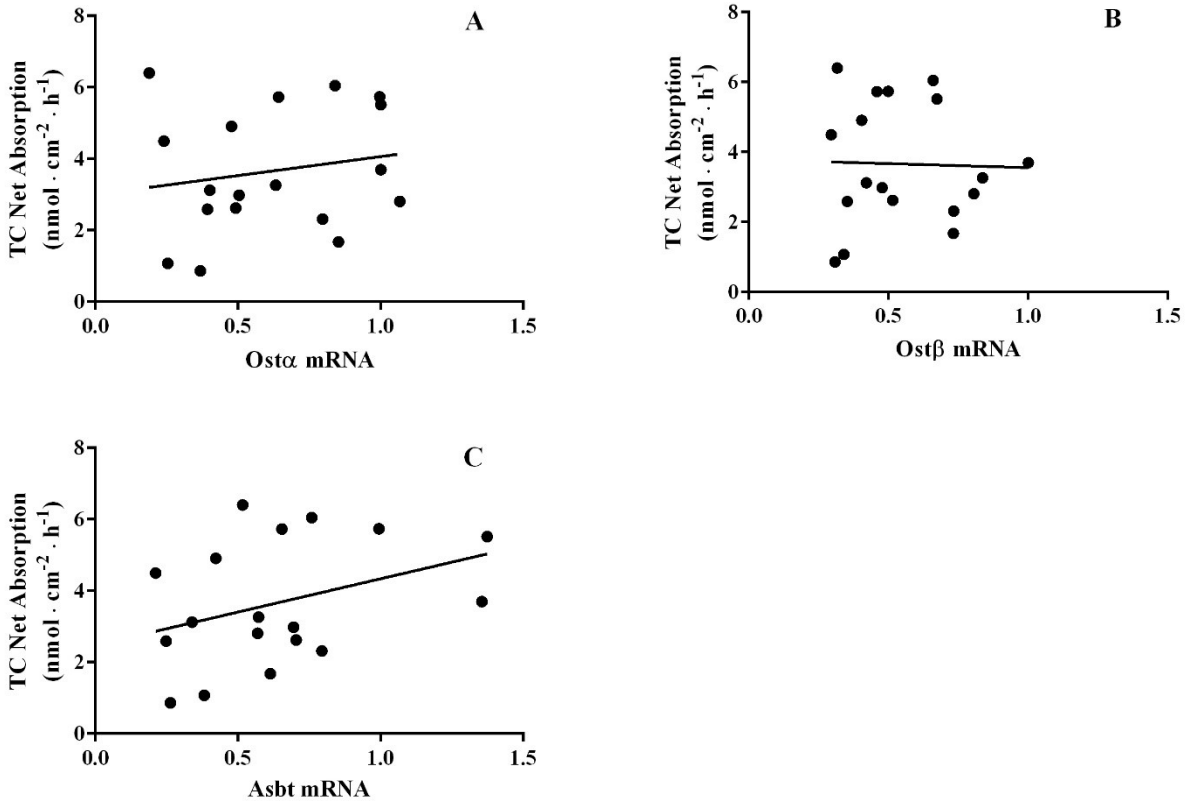

Figure 3.5. Relative mRNA expression of Ostα (**Figure 3.5A**), Ostβ (**Figure 3.5B**) or Asbt (**Figure 3.5C**) as a function of active taurocholate absorption by the ileum in Ussing chambers from 18 different animals. The mRNA expression of Ostα, Ostβ or Asbt from a mouse of 223 days old with a frailty index of 0.1048 was set to 1, and the level of expression of the transporters in the other animals expressed relative to the level of expression in this animal. The solid line shows the linear regression analysis. There was a modest positive correlation between Asbt expression and net taurocholate absorption, which was not significant. There was no apparent relationship between Ostα or Ostβ expression and net taurocholate absorption.

FIGURE 3.6

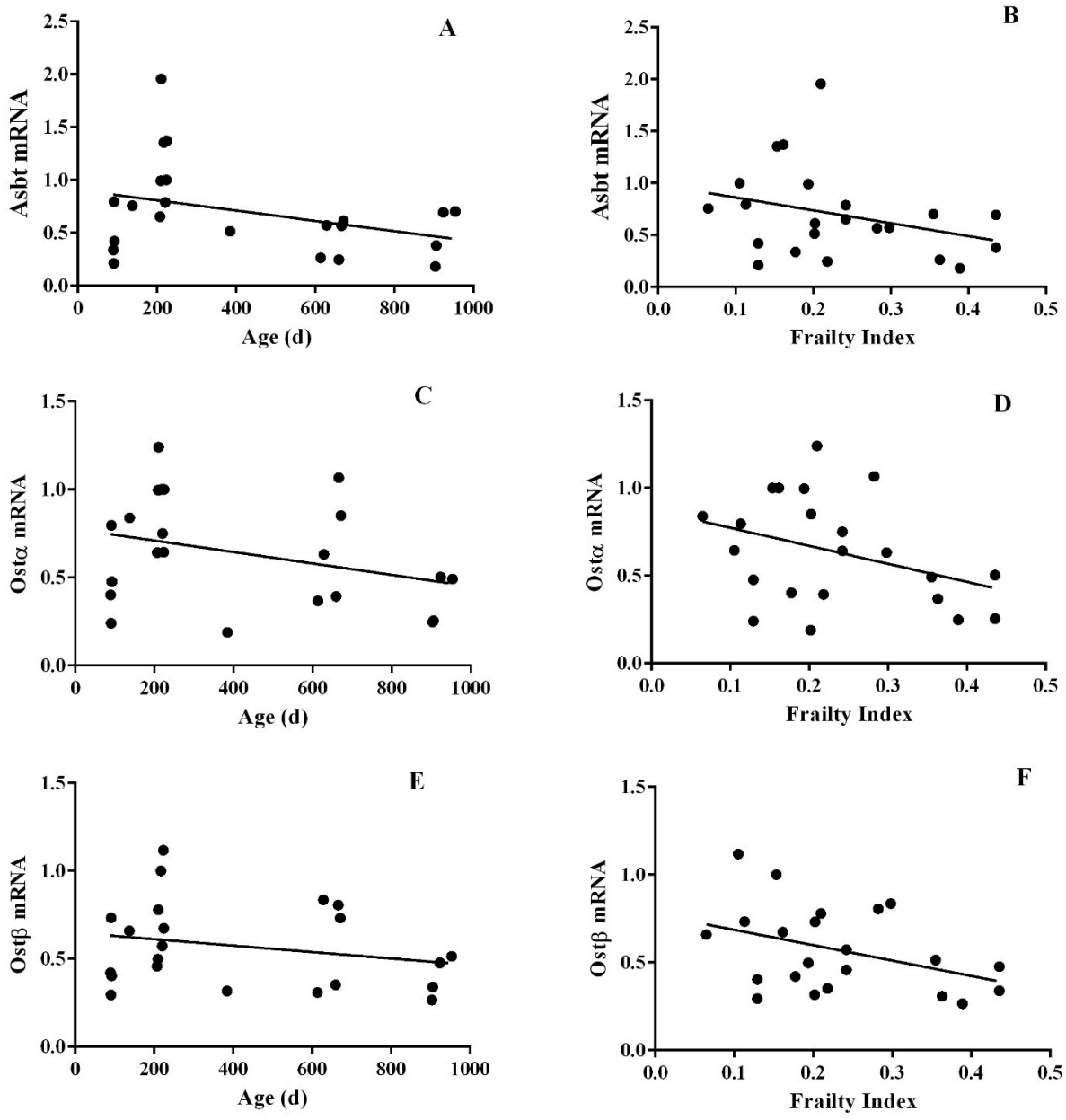
A
Asbt mRNA
Age (d)
B
Asbt mRNA
Frailty Index
C
Ostα mRNA
Age (d)
D
Ostα mRNA
Frailty Index
E
Ostβ mRNA
Age (d)
F
Ostβ mRNA
Frailty Index

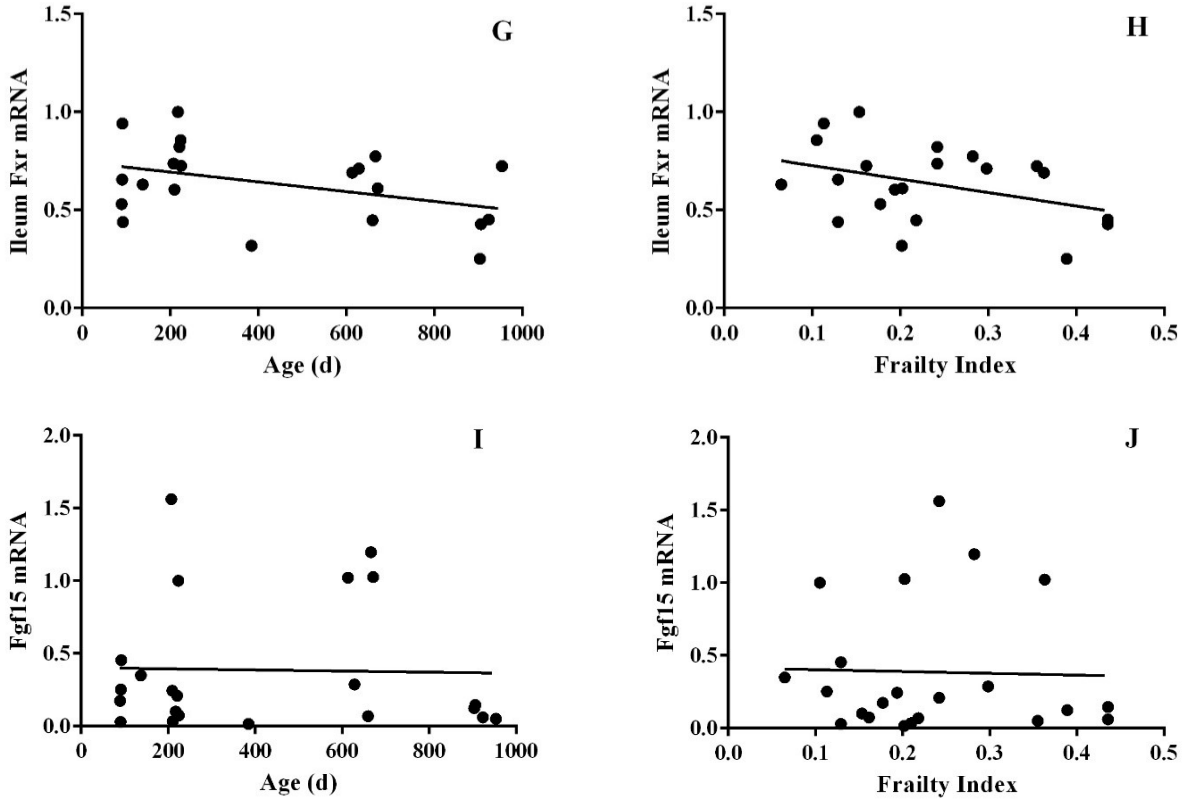

Figure 3.6. Relative mRNA expression of bile acid transporters and Fxr from the ileum of 22 mice as a function of age (A, C, E, G and I) and frailty index score (B, D, F, H and J). The mRNA expression of bile acid transporters, Fxr, and Fgf15 from a mouse of 223 days old with a frailty index of 0.1048 was set to 1, and the level of expression of the transporters and Fxr in the other animals expressed relative to the level of expression in this animal. The solid line shows the linear regression analysis. A) Asbt mRNA expression vs. age. B) Asbt mRNA expression vs. frailty index score. C) Ostα mRNA expression vs. age. D) Ostα mRNA expression vs. frailty index score. E) Ostβ mRNA expression vs. age. F) Ostβ mRNA expression vs. frailty index score. G) Fxr mRNA expression vs. age. H) Fxr mRNA expression vs. frailty index score. I) Fgf15 mRNA expression vs. age. J) Fgf15 mRNA expression vs. frailty index score.

FIGURE 3.7

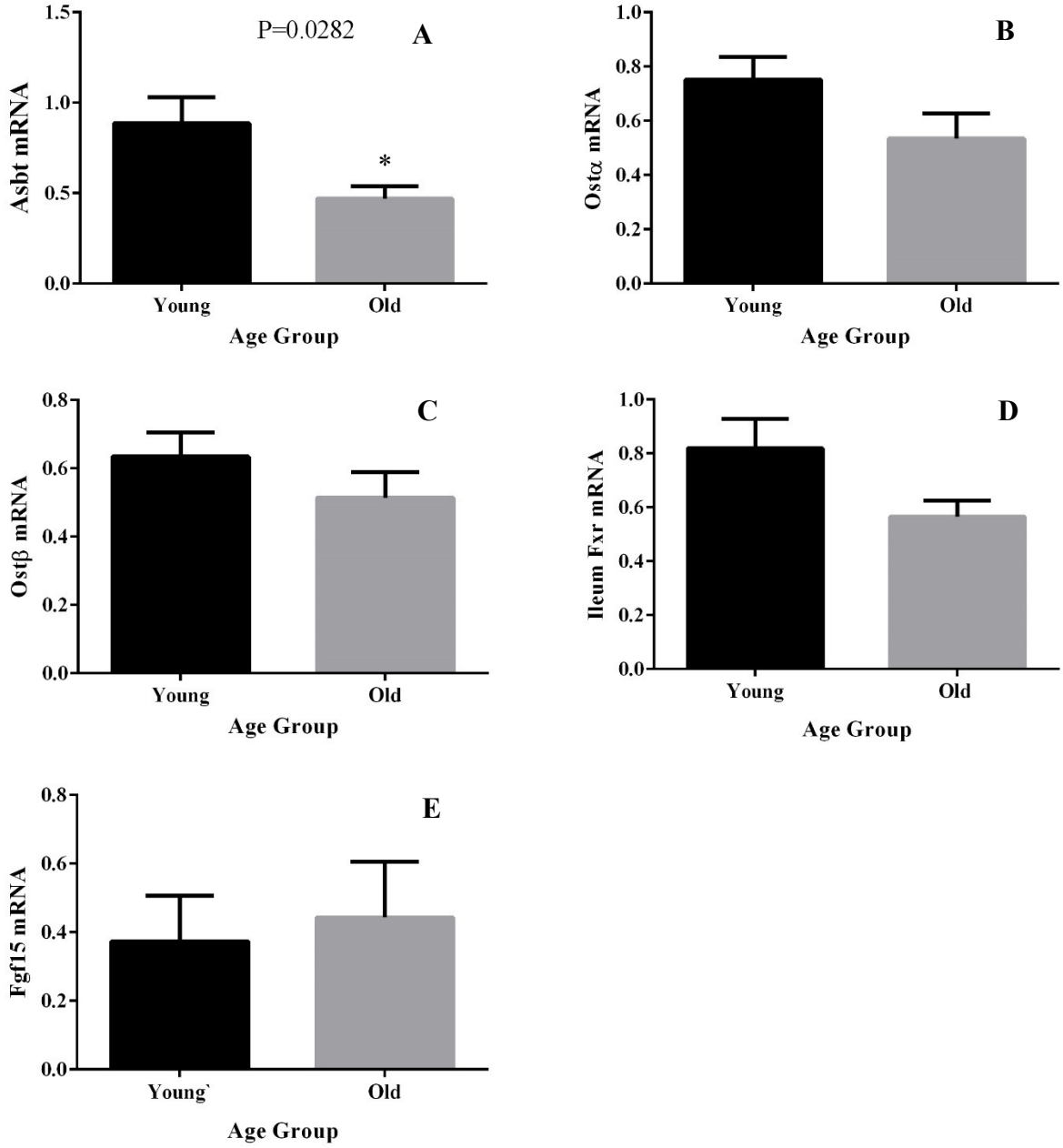

Figure 3.7. Relative mRNA expression of Asbt (A), Ostα (B), Ostβ (C), Fxr (D), and Fgf15(E) in young (~200 days old or less, n=12) and old (~600 days old or greater, n=9) mice. Data are expressed as mean ± standard error of the mean. (*, significantly different from young mice, $p<0.05$, two-tailed unpaired *t*-test)

FIGURE 3.8

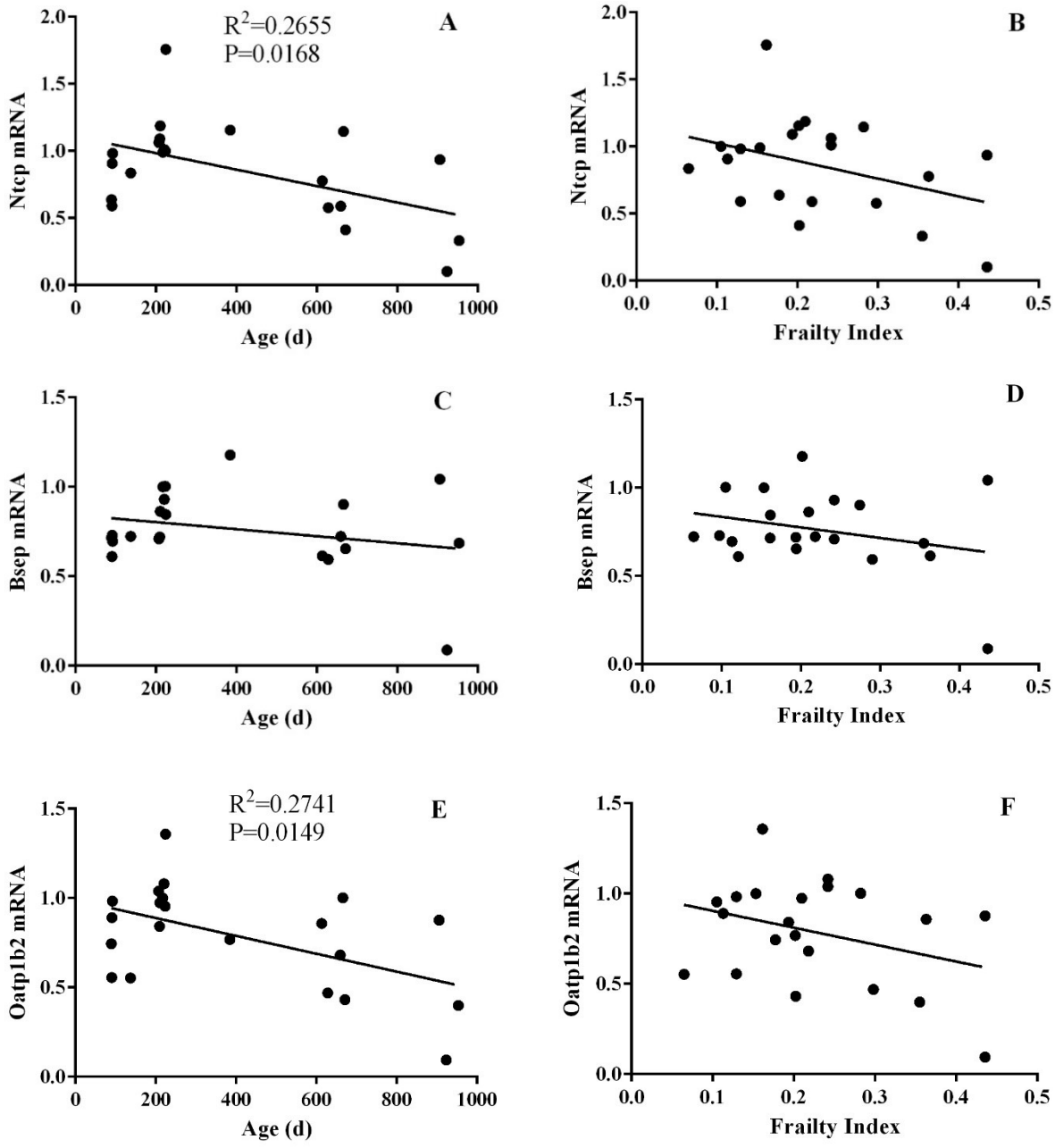
A
R^2=0.2655
P=0.0168
Ntcp mRNA
Age (d)
B
Ntcp mRNA
Frailty Index
C
Bsep mRNA
Age (d)
D
Bsep mRNA
Frailty Index
E
R^2=0.2741
P=0.0149
Oatp1b2 mRNA
Age (d)
F
Oatp1b2 mRNA
Frailty Index

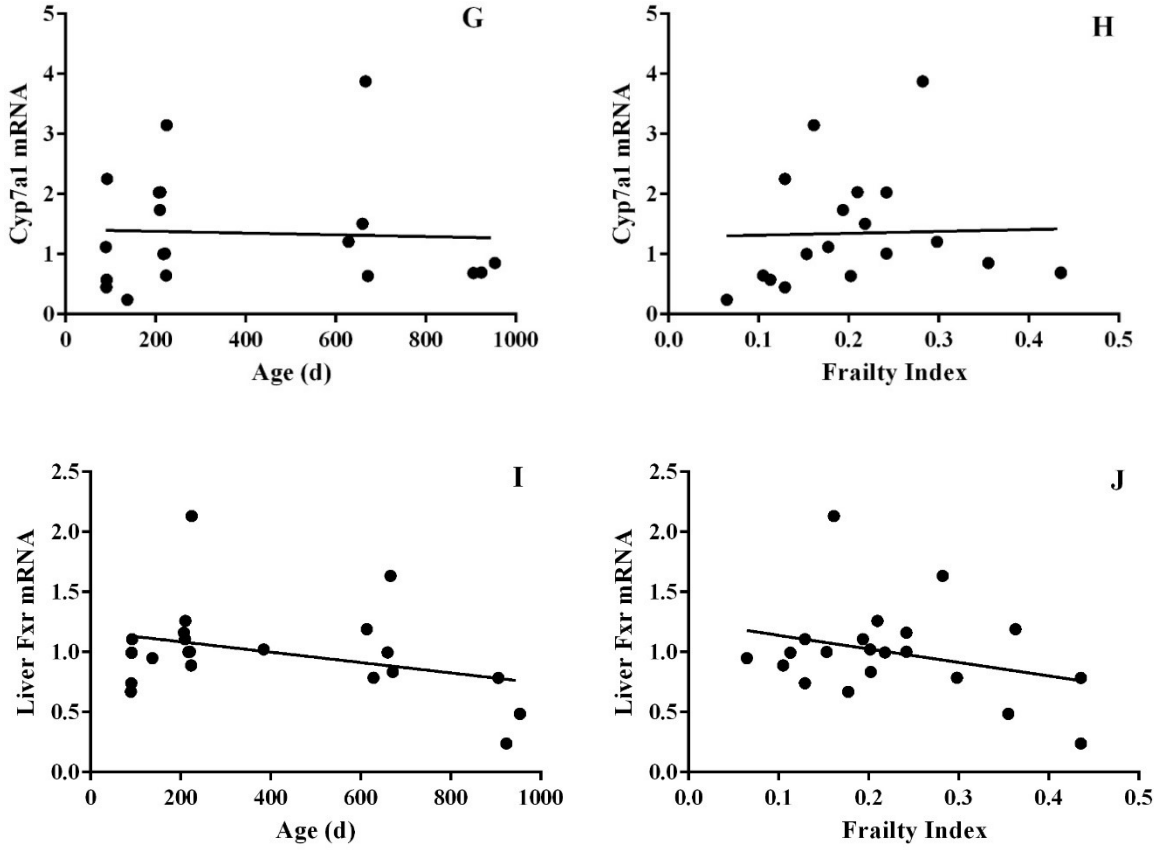

Figure 3.8. Relative mRNA expression of bile acid transporters, Fxr, and Cyp7a1 from the liver of 19-21 mice as a function of age (A, C, E, G and I) and frailty index score (B, D, F, H and J). The mRNA expression of bile acid transporters, Fxr, and Cyp7a1 from a mouse of 223 days old with a frailty index of 0.1048 was set to 1, and the level of expression of the transporters and Fxr in the other animals expressed relative to the level of expression in this animal. The solid line shows the linear regression analysis. A) Ntcp mRNA expression vs. age. B) Ntcp mRNA expression vs. frailty index score. C) Bsep mRNA expression vs. age. D) Bsep mRNA expression vs. frailty index score. E) Oatp1b2 mRNA expression vs. age. F) Oatp1b2 mRNA expression vs. frailty index score. G) Cyp7a1 mRNA expression vs. age. H) Cyp7a1 mRNA expression vs. frailty index score. I) Fxr mRNA expression vs. age. J) Fxr mRNA expression vs. frailty index score. The expression level of Ntcp and Oatp1b2 showed a significant negative linear correlation with age ($p=0.017$ and 0.015, respectively) but not with frailty index score.

FIGURE 3.9

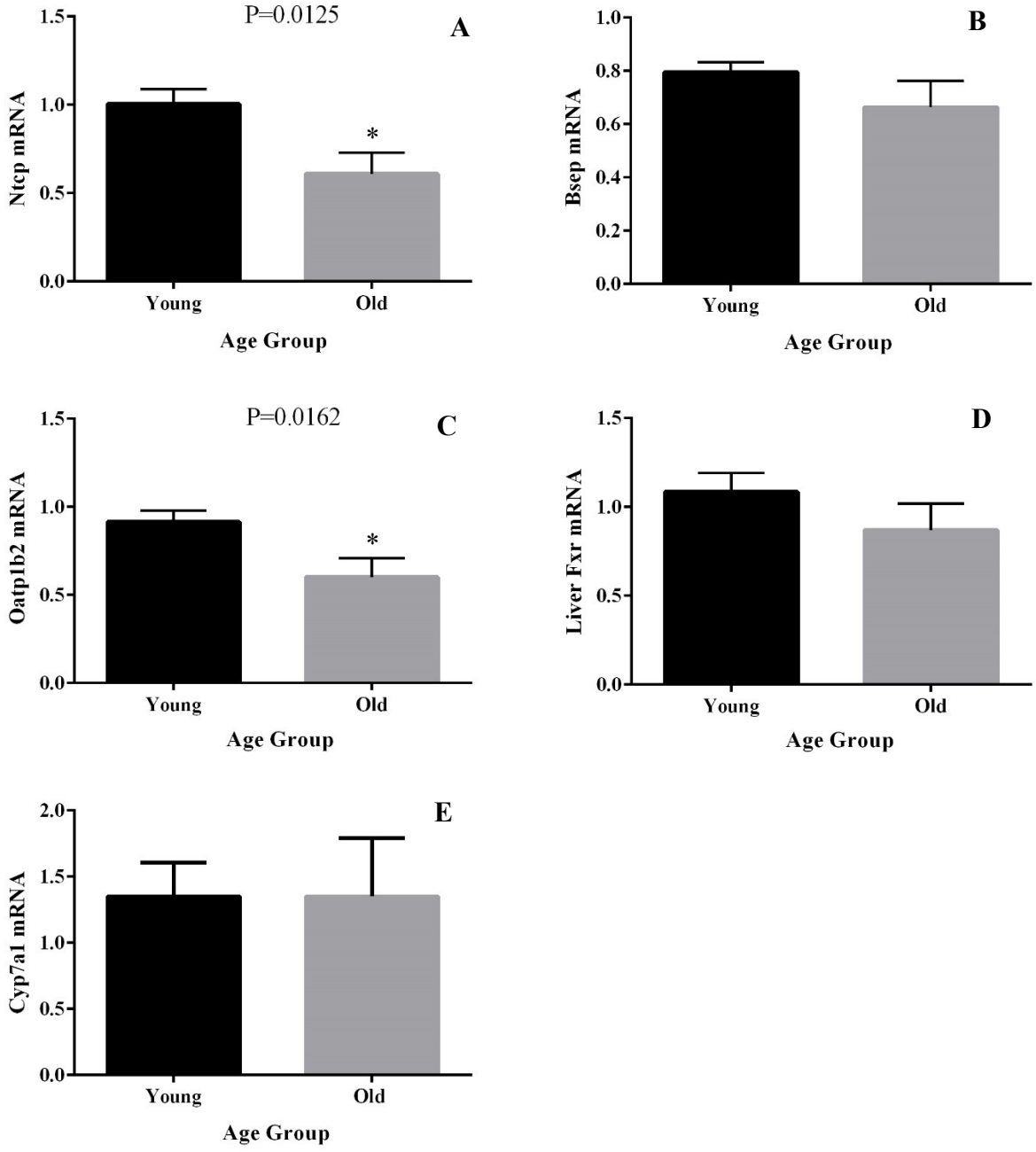

Figure 3.9. Relative mRNA expression of Ntcp (A), Bsep (B), Oatp1b2 (C), Fxr (D) and Cyp7a1 in young (~200 days old or less, n=12) and old (~600 days old or greater, n=9) mice. Data are expressed as mean ± standard error of the mean. (*, significantly different from young mice, $p<0.05$, two-tailed unpaired *t*-test)

CHAPTER 4: DISCUSSION

Bile acids serve a number of physiological roles, including the emulsification of dietary lipids and the regulation of glucose and lipid metabolism. Bile acid homeostasis is maintained in part through enterohepatic circulation of bile acids. That is, bile acids are secreted into the bile by hepatocytes, bile acids deposited into the intestinal lumen are absorbed into the hepatic portal blood by epithelial cells of the ileum, and finally, bile acids are taken up into hepatocytes from the hepatic portal blood, thereby completing one cycle of enterohepatic bile acid circulation.

The enterohepatic circulation of bile acids involves the concerted activity of multiple ileal and hepatic transporters. Specifically, ASBT at the apical membrane of terminal ileum epithelial cell and OSTα/β at the basolateral membrane are involved in intestinal bile acid absorption (intestinal lumen-to-portal vein blood) (26). At the basolateral side of hepatocytes, bile acids are taken up into the hepatocyte by NTCP, with some minor involvement of OATPs (26). Finally, bile acids are effluxed into the bile canaliculi by BSEP (26). The expression and function of these transporters are highly regulated in order to maintain bile acid homeostasis. Beyond serving as bile acid transporters, these transporters are also significant in pharmacokinetics in that they are potential sites of drug interactions (26, 126, 127), can be targeted for enhancing oral drug bioavailability or delivery of drugs to the liver (132-134, 137), and are potential pharmacological targets for treating type II diabetes (121, 124).

A limited number of studies indicate that age-related changes in bile acid homeostasis exist. Age-related changes have been described in bile acid synthesis (156), expression of bile acid transporters (152, 155), bile acid enterohepatic circulation (153), and serum bile acid levels and composition (149, 150, 152). However, none of these studies have directly measured the rate of intestinal bile acid absorption as a function of age or frailty level. Therefore, the

objective of the thesis was to directly measure the rate of bile acid transport across the terminal ileum in mice and to quantify the mRNA expression of bile acid transporters and other related genes as a function of age and frailty level.

Although several studies suggest that there are age-related changes in processes regulating bile acid enterohepatic circulation, nothing is known about the impact of frailty. Several methods of quantifying frailty have been developed for both human and mouse models (140, 141, 147, 148). We were in a unique position to test the influence of frailty on bile acid transport since our collaborator Dr. Susan Howlett (Dalhousie University, Dept. of Pharmacology) established and validated a new non-invasive frailty assessment for mice that shows similarities to the frailty assessment established for clinical use in humans (148). That is, mice accumulate health deficits at a rate similar to the rate of humans (148). When we examined the relationship between age and frailty index score in 21 mice we found a strong positive exponential correlation, indicating that as mice get older there is a tendency for them to be frailer. The slope of the regression curve (0.013) is lower than the slope shown in the earlier study (0.038) that established the non-invasive frailty assessment method for mice (148). A possible explanation includes sex differences in deficit accumulation. Our cohort consisted of male mice exclusively, whereas the initial study was conducted with female mice. Males have a slower rate of deficit accumulation than their female counterparts in both mice and humans (148, 160), which is consistent with the lower rate of deficit accumulation in our study with male mice compared to the previous study with female mice (148). The relationship between age and frailty index score could also be fit using a linear function. Interestingly, unpublished data from the Howlett laboratory also suggest that the relationship between age and frailty in mice may be linear as opposed to exponential. Clearly, more studies with a larger cohort of both female and

male mice are needed to determine if the relationship is linear or exponential. Extrapolation of both the exponential and linear curves back to zero age in days suggested a positive frailty index score at birth. The youngest animal in our cohort was ~3 months of age. Perhaps the curve of our regression line between age and frailty index score would have been influenced if we had included younger animals (< 3 months). It is also possible that at a very young age the mice already have indications of frailty based on the examined signs of deterioration. Importantly, our data confirm other studies showing that as mice get older they become frailer.

A major objective was to directly measure the rate of intestinal bile acid absorption as a function of age and frailty level. The rate of taurocholate transport across the freshly dissected mouse ileum in Ussing chambers was determined under voltage-clamped conditions, which allowed us to determine 'active' transporter-mediated bile acid transport, and negate the contribution of passive paracellular and transcellular diffusion to taurocholate absorption. There was a significant negative linear correlation between the net taurocholate absorption rate and age, as well as frailty index score. These data indicate that there is a decrease in intestinal bile acid absorption with increasing age, and with increasing frailty level. A question is how much do age and frailty individually contribute to the change in bile acid absorption. To answer this question, we wanted to perform either multiple linear regression analysis, or partial correlation analysis. However, our data violated one assumption with each statistical test, thereby not allowing us to make conclusions based on the results of these tests. Moving forward we need to examine more animals in the age range of 200-600 days of age in order to satisfy the assumption of normality of age for testing the effects on bile acid transport of age while controlling for frailty, and for frailty while controlling for age by partial correlation analysis.

Interestingly, the highest rate of net taurocholate absorption was ~7.5 times greater than the lowest rate, which likely contributes to a reduced intestinal bile acid absorption in older and frailer individuals *in vivo*. Presumably, to counteract the reduced intestinal bile acid absorption and maintain bile acid homeostasis, there would need to be increased hepatic bile acid synthesis or reduced hepatic bile acid secretion into the bile canaliculi. Within the liver, there was no effect of age or frailty on the expression level of Cyp7a1, the rate-limiting enzyme involved in the major pathway for the synthesis of primary bile acids. Fu et al. (152) observed an increase in hepatic Cyp7a1 mRNA levels in male mice ranging from 3 months to 18 months of age. It is not clear why we did not observe a similar increase in Cyp7a1 levels. There was an effect of age on the expression level of Ntcp and Oatp1b2 mRNA in the liver, with a lower expression in older animals compared to young animals. These findings are consistent with a previous study, where the expression of both Ntcp and Oatp1b2 mRNA was lower in old male mice (~24 months of age) compared to young male mice (~12 months of age) (155). However, another study found no apparent effect of aging on Ntcp or Oatp1b2 mRNA expression in the liver of male mice, even though they did observe lower protein expression of Ntcp and Oatp1b2 protein by immunoblotting in 27-month-old female mice compared to 3-month-olds (152). Bsep also contributes to biliary secretion of bile acids, but we found no significant change in Bsep expression with age or frailty level. Fu et al. (152) also did not observe a change in Bsep expression with increasing age in male mice, whereas Zhang et al. (155) found lower hepatic expression of Bsep mRNA in livers of male mice of 24 months of age compared to animals of 12 months of age. Together, our data and those of others suggest that the hepatic expression of bile acid transporters is likely reduced in older individuals, possibly leading to reduced biliary secretion of bile acids.

One possible explanation for the decreased bile acid absorption in terminal ileum with increasing age and frailty level is a reduced expression of the major intestinal bile acid transporters, Asbt and Ostα/β. To determine if Asbt, Ostα or Ostβ mRNA expression levels are predictive of bile acid absorption, we plotted the mRNA expression level of each gene against the taurocholate net absorption rate. Although there were modest positive correlations between Asbt and Ostα mRNA expression and the taurocholate net absorption rate, the effects were not significant, indicating that mRNA expression of the intestinal bile acid transporters is not predictive of the taurocholate net absorption rate. There are several possible explanations for these results. First, mRNA expression of the transporters may not reflect their level of protein expression or activity in the plasma membrane. Unfortunately, there was not enough ileum from each animal in order to examine protein expression by immunoblotting, i.e., all of the tissue was used for functional and qPCR experiments. Second, the terminal ileum from a mouse is extremely small, and hence, the expression level of the transporters in the tissue used for transport measurement and that used for mRNA expression analysis could be different. Third, since the intestinal absorption of bile acids is dependent on Asbt and Ostα/β working in series (i.e., one at the apical membrane and the other at the basolateral membrane), modest changes in the expression of both could result in significant changes in the rate of absorption. That is, by only looking at taurocholate net absorption rate as a function of the expression of the uptake pathway or the efflux pathway individually, we may be overlooking the combined effect of each on overall function. Not surprising given the fact that mRNA expression of Asbt, Ostα and Ostβ were not predictive of the rate of taurocholate absorption, there was no significant linear relationship between Asbt, Ostα or Ostβ with age or frailty level. However, the trends for each were that of decreasing levels of mRNA expression with increasing age and frailty index score.

However, when we analyzed the mRNA expression of Asbt in the older vs. younger cohort by *t*-test, there was a significantly lower level of Asbt in the old vs. young mice, which is consistent with the significantly lower rate of intestinal taurocholate transport in the old vs. young mice.

Fxr and Fgf15 are important factors influencing the expression of bile acid transporters and Cyp7a1. The mRNA expression of Fxr in the intestine and liver showed a slight decrease with both increasing age and frailty level, which was not significant. There was no relationship between intestinal Fgf15 mRNA level and age or frailty level. Fu et al. also showed in male mice that Fxr mRNA expression in the liver does not change with increasing age, and there was also relatively little change in the expression of Fgf15 from 6 months to 27 months of age. This indicates that although there is a considerable change in bile acid absorption by the terminal ileum with increasing age and frailty level, the mRNA expression of regulators of bile acid transporters and Cyp7a1 remains relatively stable.

The change in bile acid absorption by the terminal ileum and the expression of intestinal and hepatic bile acid transporters may also influence the pharmacokinetics of therapeutic drugs. Bile acid-drug conjugates are under investigation in order to achieve higher oral bioavailability by high-jacking ASBT in the ileum and for targeted delivery of drugs to the liver by high-jacking NTCP. There is also the possibility that drugs on the market are substrates of intestinal and hepatic bile acid transporters. For example, OATPs are very important for pharmacokinetics of a variety of marketed therapeutic drugs. Reduced activity of intestinal bile acid transporters, could cause reduced oral bioavailability for drugs that are substrates of these transporters. Also, the lower expression of hepatic Ntcp and Oatp1b2 levels could lead to reduced hepatic uptake and elimination of drugs. Since pharmacological inhibition of ASBT has a blood glucose lowering effect, perhaps its lower expression in the old versus young contributes to the increased

incidence of hypoglycemia in the geriatric population(161). Further work is required to determine if aging and frailty influence the pharmacokinetics of substrates of intestinal and hepatic bile acid transporters.

There were several limitations in this study. 1) The experimental mice underwent two different euthanasia procedures (see "Materials and Methods"). In addition, the use of carbachol, a muscarinic agonist, in the second euthanasia procedure may influence intestinal functions. However, there was no difference in the age, frailty index, intestinal bile acid absorption, or gene expression levels between the two groups of animals (data not shown). 2) This study only involved male mice due to a limited access to female mice. As described above, gender differences exist in frailty and bile acid metabolism. 3) Mice of ~400 days old were not available. 4) The tissue obtained for gene expression analysis was more proximal to the tissue obtained for bile acid transport experiment. It is possible that the gene expression pattern may change in different segments of the GI tract. Also the protein expression may not directly reflect mRNA levels. However, there was not enough ileum tissue to perform a Western blot analysis. 5) A limited sample size may decrease the reliability of the results. 6) There are differences in bile acid metabolism and frailty between mice and human, thus, caution needs to be taken when extrapolating the results to human.

In summary, we found that the rate of active bile acid absorption by the ileum decreases with increasing age and frailty. The mRNA expression of Asbt was lower in older animals compared to younger animals, and this corresponded to a lower rate of ileal bile acid absorption in older animals. The expression of the hepatic bile acid uptake transporters Ntcp and Oatp1b2 also decreased with increasing age and frailty. These data suggest that the overall capacity for enterohepatic bile acid circulation is lower in older frailer adults. This could impact the normal

physiological function of bile acids, as well as the pharmacokinetics of drugs that are substrates of bile acid transporters.

REFERENCES

1. Chiang JY. Bile acid metabolism and signaling. Comprehensive Physiology. 2013;3(3):1191-212.
2. Hofmann AF. The continuing importance of bile acids in liver and intestinal disease. Archives of internal medicine. 1999;159(22):2647-58.
3. Russell DW. The enzymes, regulation, and genetics of bile acid synthesis. Annual review of biochemistry. 2003;72:137-74.
4. Monte M-J. Bile acids: Chemistry, physiology, and pathophysiology. World Journal of Gastroenterology. 2009;15(7):804.
5. Schwarz M, Russell DW, Dietschy JM, Turley SD. Marked reduction in bile acid synthesis in cholesterol 7alpha-hydroxylase-deficient mice does not lead to diminished tissue cholesterol turnover or to hypercholesterolemia. Journal of lipid research. 1998;39(9):1833-43.
6. Duane WC, Javitt NB. 27-hydroxycholesterol: production rates in normal human subjects. Journal of lipid research. 1999;40(7):1194-9.
7. Aldini R, Roda A, Lenzi P, Calcaterra D, Vaccari C, Calzolari M, et al. Hepatic uptake and biliary secretion of bile acids in the perfused rat liver. Pharmacological research. 1992;25(1):51-61.
8. Hofmann AF. The Function of Bile Salts in Fat Absorption. The Solvent Properties of Dilute Micellar Solutions of Conjugated Bile Salts. The Biochemical journal. 1963;89:57-68.
9. Pandak WM, Vlahcevic ZR, Heuman DM, Redford KS, Chiang JY, Hylemon PB. Effects of different bile salts on steady-state mRNA levels and transcriptional activity of cholesterol 7 alpha-hydroxylase. Hepatology. 1994;19(4):941-7.
10. Heuman DM, Hylemon PB, Vlahcevic ZR. Regulation of bile acid synthesis. III. Correlation between biliary bile salt hydrophobicity index and the activities of enzymes regulating cholesterol and bile acid synthesis in the rat. Journal of lipid research. 1989;30(8):1161-71.
11. Hylemon PB, Zhou H, Pandak WM, Ren S, Gil G, Dent P. Bile acids as regulatory molecules. Journal of lipid research. 2009;50(8):1509-20.
12. Ding L, Yang L, Wang Z, Huang W. Bile acid nuclear receptor FXR and digestive system diseases. Acta pharmaceutica Sinica B. 2015;5(2):135-44.
13. Goodwin B, Jones SA, Price RR, Watson MA, McKee DD, Moore LB, et al. A regulatory cascade of the nuclear receptors FXR, SHP-1, and LRH-1 represses bile acid biosynthesis. Molecular cell. 2000;6(3):517-26.
14. Lu TT, Makishima M, Repa JJ, Schoonjans K, Kerr TA, Auwerx J, et al. Molecular basis for feedback regulation of bile acid synthesis by nuclear receptors. Molecular cell. 2000;6(3):507-15.
15. Hayhurst GP, Lee YH, Lambert G, Ward JM, Gonzalez FJ. Hepatocyte nuclear factor 4alpha (nuclear receptor 2A1) is essential for maintenance of hepatic gene expression and lipid homeostasis. Molecular and cellular biology. 2001;21(4):1393-403.
16. Zhang M, Chiang JY. Transcriptional regulation of the human sterol 12alpha-hydroxylase gene (CYP8B1): roles of heaptocyte nuclear factor 4alpha in mediating bile acid repression. The Journal of biological chemistry. 2001;276(45):41690-9.

17. Inagaki T, Choi M, Moschetta A, Peng L, Cummins CL, McDonald JG, et al. Fibroblast growth factor 15 functions as an enterohepatic signal to regulate bile acid homeostasis. Cell metabolism. 2005;2(4):217-25.
18. Holt JA, Luo G, Billin AN, Bisi J, McNeill YY, Kozarsky KF, et al. Definition of a novel growth factor-dependent signal cascade for the suppression of bile acid biosynthesis. Genes & development. 2003;17(13):1581-91.
19. Lee YK, Schmidt DR, Cummins CL, Choi M, Peng L, Zhang Y, et al. Liver receptor homolog-1 regulates bile acid homeostasis but is not essential for feedback regulation of bile acid synthesis. Molecular endocrinology. 2008;22(6):1345-56.
20. Mataki C, Magnier BC, Houten SM, Annicotte JS, Argmann C, Thomas C, et al. Compromised intestinal lipid absorption in mice with a liver-specific deficiency of liver receptor homolog 1. Molecular and cellular biology. 2007;27(23):8330-9.
21. Kim I, Ahn SH, Inagaki T, Choi M, Ito S, Guo GL, et al. Differential regulation of bile acid homeostasis by the farnesoid X receptor in liver and intestine. Journal of lipid research. 2007;48(12):2664-72.
22. Pellicoro A, Faber KN. Review article: The function and regulation of proteins involved in bile salt biosynthesis and transport. Alimentary pharmacology & therapeutics. 2007;26 Suppl 2:149-60.
23. Chiang JY. Bile acids: regulation of synthesis. Journal of lipid research. 2009;50(10):1955-66.
24. Shneider BL, Dawson PA, Christie DM, Hardikar W, Wong MH, Suchy FJ. Cloning and molecular characterization of the ontogeny of a rat ileal sodium-dependent bile acid transporter. The Journal of clinical investigation. 1995;95(2):745-54.
25. Craddock AL, Love MW, Daniel RW, Kirby LC, Walters HC, Wong MH, et al. Expression and transport properties of the human ileal and renal sodium-dependent bile acid transporter. The American journal of physiology. 1998;274(1 Pt 1):G157-69.
26. Dawson PA, Lan T, Rao A. Bile acid transporters. Journal of lipid research. 2009;50(12):2340-57.
27. Dawson PA, Haywood J, Craddock AL, Wilson M, Tietjen M, Kluckman K, et al. Targeted deletion of the ileal bile acid transporter eliminates enterohepatic cycling of bile acids in mice. The Journal of biological chemistry. 2003;278(36):33920-7.
28. Weinman SA, Carruth MW, Dawson PA. Bile acid uptake via the human apical sodium-bile acid cotransporter is electrogenic. The Journal of biological chemistry. 1998;273(52):34691-5.
29. Kramer W, Stengelin S, Baringhaus KH, Enhsen A, Heuer H, Becker W, et al. Substrate specificity of the ileal and the hepatic Na(+)/bile acid cotransporters of the rabbit. I. Transport studies with membrane vesicles and cell lines expressing the cloned transporters. Journal of lipid research. 1999;40(9):1604-17.
30. Seward DJ, Koh AS, Boyer JL, Ballatori N. Functional complementation between a novel mammalian polygenic transport complex and an evolutionarily ancient organic solute transporter, OSTalpha-OSTbeta. The Journal of biological chemistry. 2003;278(30):27473-82.
31. Dawson PA, Hubbert M, Haywood J, Craddock AL, Zerangue N, Christian WV, et al. The heteromeric organic solute transporter alpha-beta, Ostalpha-Ostbeta, is an ileal basolateral bile acid transporter. The Journal of biological chemistry. 2005;280(8):6960-8.
32. Rao A, Haywood J, Craddock AL, Belinsky MG, Kruh GD, Dawson PA. The organic solute transporter alpha-beta, Ostalpha-Ostbeta, is essential for intestinal bile acid transport and

homeostasis. Proceedings of the National Academy of Sciences of the United States of America. 2008;105(10):3891-6.
33. Van Dyke RW, Stephens JE, Scharschmidt BF. Bile acid transport in cultured rat hepatocytes. The American journal of physiology. 1982;243(6):G484-92.
34. Kouzuki H, Suzuki H, Ito K, Ohashi R, Sugiyama Y. Contribution of sodium taurocholate co-transporting polypeptide to the uptake of its possible substrates into rat hepatocytes. The Journal of pharmacology and experimental therapeutics. 1998;286(2):1043-50.
35. Wolkoff AW. Organic anion uptake by hepatocytes. Comprehensive Physiology. 2014;4(4):1715-35.
36. Kouzuki H, Suzuki H, Ito K, Ohashi R, Sugiyama Y. Contribution of organic anion transporting polypeptide to uptake of its possible substrates into rat hepatocytes. The Journal of pharmacology and experimental therapeutics. 1999;288(2):627-34.
37. Stieger B, Meier Y, Meier PJ. The bile salt export pump. Pflugers Archiv : European journal of physiology. 2007;453(5):611-20.
38. Zelcer N, Saeki T, Bot I, Kuil A, Borst P. Transport of bile acids in multidrug-resistance-protein 3-overexpressing cells co-transfected with the ileal Na+-dependent bile-acid transporter. The Biochemical journal. 2003;369(Pt 1):23-30.
39. Zelcer N, Reid G, Wielinga P, Kuil A, van der Heijden I, Schuetz JD, et al. Steroid and bile acid conjugates are substrates of human multidrug-resistance protein (MRP) 4 (ATP-binding cassette C4). The Biochemical journal. 2003;371(Pt 2):361-7.
40. Zollner G, Fickert P, Silbert D, Fuchsbichler A, Marschall H-U, Zatloukal K, et al. Adaptive changes in hepatobiliary transporter expression in primary biliary cirrhosis. Journal of Hepatology. 2003;38(6):717-27.
41. Keitel V, Burdelski M, Warskulat U, Kuhlkamp T, Keppler D, Haussinger D, et al. Expression and localization of hepatobiliary transport proteins in progressive familial intrahepatic cholestasis. Hepatology. 2005;41(5):1160-72.
42. Ananthanarayanan M, Ng OC, Boyer JL, Suchy FJ. Characterization of cloned rat liver Na(+)-bile acid cotransporter using peptide and fusion protein antibodies. The American journal of physiology. 1994;267(4 Pt 1):G637-43.
43. Meier PJ, Eckhardt U, Schroeder A, Hagenbuch B, Stieger B. Substrate specificity of sinusoidal bile acid and organic anion uptake systems in rat and human liver. Hepatology. 1997;26(6):1667-77.
44. Wong MH, Oelkers P, Craddock AL, Dawson PA. Expression cloning and characterization of the hamster ileal sodium-dependent bile acid transporter. The Journal of biological chemistry. 1994;269(2):1340-7.
45. Boyer JL, Ng OC, Ananthanarayanan M, Hofmann AF, Schteingart CD, Hagenbuch B, et al. Expression and characterization of a functional rat liver Na+ bile acid cotransport system in COS-7 cells. The American journal of physiology. 1994;266(3 Pt 1):G382-7.
46. Hagenbuch B, Meier PJ. Sinusoidal (basolateral) bile salt uptake systems of hepatocytes. Seminars in liver disease. 1996;16(2):129-36.
47. Kosters A, Karpen SJ. Bile acid transporters in health and disease. Xenobiotica; the fate of foreign compounds in biological systems. 2008;38(7-8):1043-71.
48. Stieger B, O'Neill B, Meier PJ. ATP-dependent bile-salt transport in canalicular rat liver plasma-membrane vesicles. The Biochemical journal. 1992;284 (Pt 1):67-74.
49. Childs S, Yeh RL, Georges E, Ling V. Identification of a sister gene to P-glycoprotein. Cancer research. 1995;55(10):2029-34.

50. Gerloff T, Stieger B, Hagenbuch B, Madon J, Landmann L, Roth J, et al. The sister of P-glycoprotein represents the canalicular bile salt export pump of mammalian liver. The Journal of biological chemistry. 1998;273(16):10046-50.
51. Byrne JA, Strautnieks SS, Mieli–Vergani G, Higgins CF, Linton KJ, Thompson RJ. The human bile salt export pump: Characterization of substrate specificity and identification of inhibitors. Gastroenterology. 2002;123(5):1649-58.
52. Noé J, Stieger B, Meier PJ. Functional expression of the canalicular bile salt export pump of human liver. Gastroenterology. 2002;123(5):1659-66.
53. Strautnieks SS, Bull LN, Knisely AS, Kocoshis SA, Dahl N, Arnell H, et al. A gene encoding a liver-specific ABC transporter is mutated in progressive familial intrahepatic cholestasis. Nature genetics. 1998;20(3):233-8.
54. Chen F, Ma L, Dawson PA, Sinal CJ, Sehayek E, Gonzalez FJ, et al. Liver receptor homologue-1 mediates species- and cell line-specific bile acid-dependent negative feedback regulation of the apical sodium-dependent bile acid transporter. The Journal of biological chemistry. 2003;278(22):19909-16.
55. Neimark E, Chen F, Li X, Shneider BL. Bile acid-induced negative feedback regulation of the human ileal bile acid transporter. Hepatology. 2004;40(1):149-56.
56. Sinha J, Chen F, Miloh T, Burns RC, Yu Z, Shneider BL. beta-Klotho and FGF-15/19 inhibit the apical sodium-dependent bile acid transporter in enterocytes and cholangiocytes. American journal of physiology Gastrointestinal and liver physiology. 2008;295(5):G996-G1003.
57. Frankenberg T, Rao A, Chen F, Haywood J, Shneider BL, Dawson PA. Regulation of the mouse organic solute transporter alpha-beta, Ostalpha-Ostbeta, by bile acids. American journal of physiology Gastrointestinal and liver physiology. 2006;290(5):G912-22.
58. Lee H, Zhang Y, Lee FY, Nelson SF, Gonzalez FJ, Edwards PA. FXR regulates organic solute transporters alpha and beta in the adrenal gland, kidney, and intestine. Journal of lipid research. 2006;47(1):201-14.
59. Zollner G, Wagner M, Moustafa T, Fickert P, Silbert D, Gumhold J, et al. Coordinated induction of bile acid detoxification and alternative elimination in mice: role of FXR-regulated organic solute transporter-alpha/beta in the adaptive response to bile acids. American journal of physiology Gastrointestinal and liver physiology. 2006;290(5):G923-32.
60. Denson LA, Sturm E, Echevarria W, Zimmerman TL, Makishima M, Mangelsdorf DJ, et al. The Orphan Nuclear Receptor, shp, Mediates Bile Acid-Induced Inhibition of the Rat Bile Acid Transporter, ntcp. Gastroenterology. 2001;121(1):140-7.
61. Jung D, Hagenbuch B, Fried M, Meier PJ, Kullak-Ublick GA. Role of liver-enriched transcription factors and nuclear receptors in regulating the human, mouse, and rat NTCP gene. American journal of physiology Gastrointestinal and liver physiology. 2004;286(5):G752-61.
62. Wang L, Lee YK, Bundman D, Han Y, Thevananther S, Kim CS, et al. Redundant pathways for negative feedback regulation of bile acid production. Developmental cell. 2002;2(6):721-31.
63. Ananthanarayanan M, Balasubramanian N, Makishima M, Mangelsdorf DJ, Suchy FJ. Human bile salt export pump promoter is transactivated by the farnesoid X receptor/bile acid receptor. The Journal of biological chemistry. 2001;276(31):28857-65.
64. Zollner G, Fickert P, Fuchsbichler A, Silbert D, Wagner M, Arbeiter S, et al. Role of nuclear bile acid receptor, FXR, in adaptive ABC transporter regulation by cholic and

ursodeoxycholic acid in mouse liver, kidney and intestine. Journal of Hepatology. 2003;39(4):480-8.
65. Jung D, Fried M, Kullak-Ublick GA. Human apical sodium-dependent bile salt transporter gene (SLC10A2) is regulated by the peroxisome proliferator-activated receptor alpha. The Journal of biological chemistry. 2002;277(34):30559-66.
66. Chen X, Chen F, Liu S, Glaeser H, Dawson PA, Hofmann AF, et al. Transactivation of rat apical sodium-dependent bile acid transporter and increased bile acid transport by 1alpha,25-dihydroxyvitamin D3 via the vitamin D receptor. Molecular pharmacology. 2006;69(6):1913-23.
67. Jung D, Fantin AC, Scheurer U, Fried M, Kullak-Ublick GA. Human ileal bile acid transporter gene ASBT (SLC10A2) is transactivated by the glucocorticoid receptor. Gut. 2004;53(1):78-84.
68. Green RM, Beier D, Gollan JL. Regulation of hepatocyte bile salt transporters by endotoxin and inflammatory cytokines in rodents. Gastroenterology. 1996;111(1):193-8.
69. Le Vee M, Lecureur V, Stieger B, Fardel O. Regulation of drug transporter expression in human hepatocytes exposed to the proinflammatory cytokines tumor necrosis factor-alpha or interleukin-6. Drug metabolism and disposition: the biological fate of chemicals. 2009;37(3):685-93.
70. Moseley RH. Sepsis-associated cholestasis. Gastroenterology. 1997;112(1):302-6.
71. Lee JM, Trauner M, Soroka CJ, Stieger B, Meier PJ, Boyer JL. Expression of the bile salt export pump is maintained after chronic cholestasis in the rat. Gastroenterology. 2000;118(1):163-72.
72. Zinchuk V, Zinchuk O, Okada T. Experimental LPS-induced cholestasis alters subcellular distribution and affects colocalization of Mrp2 and Bsep proteins: a quantitative colocalization study. Microscopy research and technique. 2005;67(2):65-70.
73. Eloranta JJ, Jung D, Kullak-Ublick GA. The human Na+-taurocholate cotransporting polypeptide gene is activated by glucocorticoid receptor and peroxisome proliferator-activated receptor-gamma coactivator-1alpha, and suppressed by bile acids via a small heterodimer partner-dependent mechanism. Molecular endocrinology. 2006;20(1):65-79.
74. Cao J, Gowri PM, Ganguly TC, Wood M, Hyde JF, Talamantes F, et al. PRL, placental lactogen, and GH induce NA(+)/taurocholate-cotransporting polypeptide gene expression by activating signal transducer and activator of transcription-5 in liver cells. Endocrinology. 2001;142(10):4212-22.
75. Simon FR, Fortune J, Iwahashi M, Qadri I, Sutherland E. Multihormonal regulation of hepatic sinusoidal Ntcp gene expression. American journal of physiology Gastrointestinal and liver physiology. 2004;287(4):G782-94.
76. Kassam A, Miao B, Young PR, Mukherjee R. Retinoid X receptor (RXR) agonist-induced antagonism of farnesoid X receptor (FXR) activity due to absence of coactivator recruitment and decreased DNA binding. The Journal of biological chemistry. 2003;278(12):10028-32.
77. Hoeke MO, Plass JR, Heegsma J, Geuken M, van Rijsbergen D, Baller JF, et al. Low retinol levels differentially modulate bile salt-induced expression of human and mouse hepatic bile salt transporters. Hepatology. 2009;49(1):151-9.
78. Mukhopadhayay S, Ananthanarayanan M, Stieger B, Meier PJ, Suchy FJ, Anwer MS. cAMP increases liver Na+-taurocholate cotransport by translocating transporter to plasma membranes. The American journal of physiology. 1997;273(4 Pt 1):G842-8.

79. Gatmaitan ZC, Nies AT, Arias IM. Regulation and translocation of ATP-dependent apical membrane proteins in rat liver. The American journal of physiology. 1997;272(5 Pt 1):G1041-9.
80. Misra S, Varticovski L, Arias IM. Mechanisms by which cAMP increases bile acid secretion in rat liver and canalicular membrane vesicles. American journal of physiology Gastrointestinal and liver physiology. 2003;285(2):G316-24.
81. Anwer MS. Cellular regulation of hepatic bile acid transport in health and cholestasis. Hepatology. 2004;39(3):581-90.
82. Borgstrom B, Dahlqvist A, Lundh G, Sjovall J. Studies of intestinal digestion and absorption in the human. The Journal of clinical investigation. 1957;36(10):1521-36.
83. Li T, Chiang JY. Bile acids as metabolic regulators. Current opinion in gastroenterology. 2015;31(2):159-65.
84. Renga B, Mencarelli A, Vavassori P, Brancaleone V, Fiorucci S. The bile acid sensor FXR regulates insulin transcription and secretion. Biochimica et biophysica acta. 2010;1802(3):363-72.
85. Zhang Y, Lee FY, Barrera G, Lee H, Vales C, Gonzalez FJ, et al. Activation of the nuclear receptor FXR improves hyperglycemia and hyperlipidemia in diabetic mice. Proceedings of the National Academy of Sciences of the United States of America. 2006;103(4):1006-11.
86. Ma K, Saha PK, Chan L, Moore DD. Farnesoid X receptor is essential for normal glucose homeostasis. The Journal of clinical investigation. 2006;116(4):1102-9.
87. Cariou B, van Harmelen K, Duran-Sandoval D, van Dijk TH, Grefhorst A, Abdelkarim M, et al. The farnesoid X receptor modulates adiposity and peripheral insulin sensitivity in mice. The Journal of biological chemistry. 2006;281(16):11039-49.
88. Yamagata K, Daitoku H, Shimamoto Y, Matsuzaki H, Hirota K, Ishida J, et al. Bile acids regulate gluconeogenic gene expression via small heterodimer partner-mediated repression of hepatocyte nuclear factor 4 and Foxo1. The Journal of biological chemistry. 2004;279(22):23158-65.
89. Park MJ, Kong HJ, Kim HY, Kim HH, Kim JH, Cheong JH. Transcriptional repression of the gluconeogenic gene PEPCK by the orphan nuclear receptor SHP through inhibitory interaction with C/EBPalpha. The Biochemical journal. 2007;402(3):567-74.
90. Lundasen T, Galman C, Angelin B, Rudling M. Circulating intestinal fibroblast growth factor 19 has a pronounced diurnal variation and modulates hepatic bile acid synthesis in man. Journal of internal medicine. 2006;260(6):530-6.
91. Potthoff MJ, Boney-Montoya J, Choi M, He T, Sunny NE, Satapati S, et al. FGF15/19 regulates hepatic glucose metabolism by inhibiting the CREB-PGC-1alpha pathway. Cell metabolism. 2011;13(6):729-38.
92. Kir S, Beddow SA, Samuel VT, Miller P, Previs SF, Suino-Powell K, et al. FGF19 as a postprandial, insulin-independent activator of hepatic protein and glycogen synthesis. Science. 2011;331(6024):1621-4.
93. Huang X, Yang C, Luo Y, Jin C, Wang F, McKeehan WL. FGFR4 prevents hyperlipidemia and insulin resistance but underlies high-fat diet induced fatty liver. Diabetes. 2007;56(10):2501-10.
94. Ge H, Zhang J, Gong Y, Gupte J, Ye J, Weiszmann J, et al. Fibroblast growth factor receptor 4 (FGFR4) deficiency improves insulin resistance and glucose metabolism under diet-induced obesity conditions. The Journal of biological chemistry. 2014;289(44):30470-80.

95. Sinal CJ, Tohkin M, Miyata M, Ward JM, Lambert G, Gonzalez FJ. Targeted disruption of the nuclear receptor FXR/BAR impairs bile acid and lipid homeostasis. Cell. 2000;102(6):731-44.
96. Della Badia LA, Elshourbagy NA, Mousa SA. Targeting PCSK9 as a promising new mechanism for lowering low-density lipoprotein cholesterol. Pharmacology & therapeutics. 2016.
97. Langhi C, Le May C, Kourimate S, Caron S, Staels B, Krempf M, et al. Activation of the farnesoid X receptor represses PCSK9 expression in human hepatocytes. FEBS letters. 2008;582(6):949-55.
98. Hartman HB, Gardell SJ, Petucci CJ, Wang S, Krueger JA, Evans MJ. Activation of farnesoid X receptor prevents atherosclerotic lesion formation in LDLR-/- and apoE-/- mice. Journal of lipid research. 2009;50(6):1090-100.
99. Hanniman EA, Lambert G, McCarthy TC, Sinal CJ. Loss of functional farnesoid X receptor increases atherosclerotic lesions in apolipoprotein E-deficient mice. Journal of lipid research. 2005;46(12):2595-604.
100. Mencarelli A, Renga B, Distrutti E, Fiorucci S. Antiatherosclerotic effect of farnesoid X receptor. American journal of physiology Heart and circulatory physiology. 2009;296(2):H272-81.
101. Sando KR, Knight M. Nonstatin therapies for management of dyslipidemia: a review. Clinical therapeutics. 2015;37(10):2153-79.
102. Wang X, Sato R, Brown MS, Hua X, Goldstein JL. SREBP-1, a membrane-bound transcription factor released by sterol-regulated proteolysis. Cell. 1994;77(1):53-62.
103. Li T, Chiang JY. Bile acid signaling in metabolic disease and drug therapy. Pharmacol Rev. 2014;66(4):948-83.
104. Watanabe M, Houten SM, Wang L, Moschetta A, Mangelsdorf DJ, Heyman RA, et al. Bile acids lower triglyceride levels via a pathway involving FXR, SHP, and SREBP-1c. The Journal of clinical investigation. 2004;113(10):1408-18.
105. Caron S, Huaman Samanez C, Dehondt H, Ploton M, Briand O, Lien F, et al. Farnesoid X receptor inhibits the transcriptional activity of carbohydrate response element binding protein in human hepatocytes. Molecular and cellular biology. 2013;33(11):2202-11.
106. Pineda Torra I, Claudel T, Duval C, Kosykh V, Fruchart JC, Staels B. Bile acids induce the expression of the human peroxisome proliferator-activated receptor alpha gene via activation of the farnesoid X receptor. Molecular endocrinology. 2003;17(2):259-72.
107. Kast HR, Nguyen CM, Sinal CJ, Jones SA, Laffitte BA, Reue K, et al. Farnesoid X-activated receptor induces apolipoprotein C-II transcription: a molecular mechanism linking plasma triglyceride levels to bile acids. Molecular endocrinology. 2001;15(10):1720-8.
108. Maruyama T, Miyamoto Y, Nakamura T, Tamai Y, Okada H, Sugiyama E, et al. Identification of membrane-type receptor for bile acids (M-BAR). Biochemical and biophysical research communications. 2002;298(5):714-9.
109. Kawamata Y, Fujii R, Hosoya M, Harada M, Yoshida H, Miwa M, et al. A G protein-coupled receptor responsive to bile acids. The Journal of biological chemistry. 2003;278(11):9435-40.
110. Keitel V, Cupisti K, Ullmer C, Knoefel WT, Kubitz R, Haussinger D. The membrane-bound bile acid receptor TGR5 is localized in the epithelium of human gallbladders. Hepatology. 2009;50(3):861-70.

111. Keitel V, Ullmer C, Haussinger D. The membrane-bound bile acid receptor TGR5 (Gpbar-1) is localized in the primary cilium of cholangiocytes. Biological chemistry. 2010;391(7):785-9.
112. Keitel V, Donner M, Winandy S, Kubitz R, Haussinger D. Expression and function of the bile acid receptor TGR5 in Kupffer cells. Biochemical and biophysical research communications. 2008;372(1):78-84.
113. Maruyama T, Tanaka K, Suzuki J, Miyoshi H, Harada N, Nakamura T, et al. Targeted disruption of G protein-coupled bile acid receptor 1 (Gpbar1/M-Bar) in mice. The Journal of endocrinology. 2006;191(1):197-205.
114. Watanabe M, Houten SM, Mataki C, Christoffolete MA, Kim BW, Sato H, et al. Bile acids induce energy expenditure by promoting intracellular thyroid hormone activation. Nature. 2006;439(7075):484-9.
115. Katsuma S, Hirasawa A, Tsujimoto G. Bile acids promote glucagon-like peptide-1 secretion through TGR5 in a murine enteroendocrine cell line STC-1. Biochemical and biophysical research communications. 2005;329(1):386-90.
116. D'Alessio D. Is GLP-1 a hormone: Whether and When? Journal of diabetes investigation. 2016;7 Suppl 1:50-5.
117. Thomas C, Gioiello A, Noriega L, Strehle A, Oury J, Rizzo G, et al. TGR5-mediated bile acid sensing controls glucose homeostasis. Cell metabolism. 2009;10(3):167-77.
118. Cao H, Chen ZX, Wang K, Ning MM, Zou QA, Feng Y, et al. Intestinally-targeted TGR5 agonists equipped with quaternary ammonium have an improved hypoglycemic effect and reduced gallbladder filling effect. Scientific reports. 2016;6:28676.
119. Kumar DP, Rajagopal S, Mahavadi S, Mirshahi F, Grider JR, Murthy KS, et al. Activation of transmembrane bile acid receptor TGR5 stimulates insulin secretion in pancreatic beta cells. Biochemical and biophysical research communications. 2012;427(3):600-5.
120. Vettorazzi JF, Ribeiro RA, Borck PC, Branco RC, Soriano S, Merino B, et al. The bile acid TUDCA increases glucose-induced insulin secretion via the cAMP/PKA pathway in pancreatic beta cells. Metabolism: clinical and experimental. 2016;65(3):54-63.
121. Chen L, Yao X, Young A, McNulty J, Anderson D, Liu Y, et al. Inhibition of apical sodium-dependent bile acid transporter as a novel treatment for diabetes. Am J Physiol Endocrinol Metab. 2012;302(1):E68-76.
122. Dietschy JM. Mechanisms for the intestinal absorption of bile acids. Journal of lipid research. 1968;9(3):297-309.
123. Parker HE, Wallis K, le Roux CW, Wong KY, Reimann F, Gribble FM. Molecular mechanisms underlying bile acid-stimulated glucagon-like peptide-1 secretion. British journal of pharmacology. 2012;165(2):414-23.
124. Wu Y, Aquino CJ, Cowan DJ, Anderson DL, Ambroso JL, Bishop MJ, et al. Discovery of a highly potent, nonabsorbable apical sodium-dependent bile acid transporter inhibitor (GSK2330672) for treatment of type 2 diabetes. Journal of medicinal chemistry. 2013;56(12):5094-114.
125. Han X, Sun J, Wang Y, He Z. PepT1, ASBT-Linked Prodrug Strategy to Improve Oral Bioavailability and Tissue Targeting Distribution. Current drug metabolism. 2015;16(1):71-83.
126. Kim RB, Leake B, Cvetkovic M, Roden MM, Nadeau J, Walubo A, et al. Modulation by drugs of human hepatic sodium-dependent bile acid transporter (sodium taurocholate cotransporting polypeptide) activity. The Journal of pharmacology and experimental therapeutics. 1999;291(3):1204-9.

127. Dong Z, Ekins S, Polli JE. Structure-activity relationship for FDA approved drugs as inhibitors of the human sodium taurocholate cotransporting polypeptide (NTCP). Molecular pharmaceutics. 2013;10(3):1008-19.
128. Hirano M, Maeda K, Hayashi H, Kusuhara H, Sugiyama Y. Bile salt export pump (BSEP/ABCB11) can transport a nonbile acid substrate, pravastatin. The Journal of pharmacology and experimental therapeutics. 2005;314(2):876-82.
129. Stieger B, Fattinger K, Madon J, Kullak-Ublick GA, Meier PJ. Drug- and estrogen-induced cholestasis through inhibition of the hepatocellular bile salt export pump (Bsep) of rat liver. Gastroenterology. 2000;118(2):422-30.
130. Allan GM, Lindblad AJ, Comeau A, Coppola J, Hudson B, Mannarino M, et al. Simplified lipid guidelines: Prevention and management of cardiovascular disease in primary care. Canadian family physician Medecin de famille canadien. 2015;61(10):857-67, e439-50.
131. Thompson PD, Panza G, Zaleski A, Taylor B. Statin-Associated Side Effects. Journal of the American College of Cardiology. 2016;67(20):2395-410.
132. Kramer W, Wess G, Enhsen A, Bock K, Falk E, Hoffmann A, et al. Bile acid derived HMG-CoA reductase inhibitors. Biochimica et biophysica acta. 1994;1227(3):137-54.
133. Criado JJ, Dominguez MF, Medarde M, Fernandez ER, Macias RI, Marin JJ. Structural characterization, kinetic studies, and in vitro biological activity of new cis-diamminebis-cholylglycinate(O,O') Pt(II) and cis-diamminebis-ursodeoxycholate(O,O') Pt(II) complexes. Bioconjugate chemistry. 2000;11(2):167-74.
134. Dominguez MF, Macias RI, Izco-Basurko I, de La Fuente A, Pascual MJ, Criado JM, et al. Low in vivo toxicity of a novel cisplatin-ursodeoxycholic derivative (Bamet-UD2) with enhanced cytostatic activity versus liver tumors. The Journal of pharmacology and experimental therapeutics. 2001;297(3):1106-12.
135. Ballestero MR, Monte MJ, Briz O, Jimenez F, Gonzalez-San Martin F, Marin JJ. Expression of transporters potentially involved in the targeting of cytostatic bile acid derivatives to colon cancer and polyps. Biochemical pharmacology. 2006;72(6):729-38.
136. de Miranda P, Blum MR. Pharmacokinetics of acyclovir after intravenous and oral administration. The Journal of antimicrobial chemotherapy. 1983;12 Suppl B:29-37.
137. Tolle-Sander S, Lentz KA, Maeda DY, Coop A, Polli JE. Increased acyclovir oral bioavailability via a bile acid conjugate. Molecular pharmaceutics. 2004;1(1):40-8.
138. Mitnitski AB, Mogilner AJ, Rockwood K. Accumulation of deficits as a proxy measure of aging. TheScientificWorldJournal. 2001;1:323-36.
139. Clegg A, Young J, Iliffe S, Rikkert MO, Rockwood K. Frailty in elderly people. The Lancet. 2013;381(9868):752-62.
140. de Vries NM, Staal JB, van Ravensberg CD, Hobbelen JS, Olde Rikkert MG, Nijhuis-van der Sanden MW. Outcome instruments to measure frailty: a systematic review. Ageing research reviews. 2011;10(1):104-14.
141. Mitnitski A, Howlett SE, Rockwood K. Heterogeneity of Human Aging and Its Assessment. J Gerontol A Biol Sci Med Sci. 2016.
142. Searle SD, Mitnitski A, Gahbauer EA, Gill TM, Rockwood K. A standard procedure for creating a frailty index. BMC geriatrics. 2008;8:24.
143. Kulminski AM, Ukraintseva SV, Kulminskaya IV, Arbeev KG, Land K, Yashin AI. Cumulative deficits better characterize susceptibility to death in elderly people than phenotypic frailty: lessons from the Cardiovascular Health Study. Journal of the American Geriatrics Society. 2008;56(5):898-903.

144. Fried LP, Xue QL, Cappola AR, Ferrucci L, Chaves P, Varadhan R, et al. Nonlinear multisystem physiological dysregulation associated with frailty in older women: implications for etiology and treatment. J Gerontol A Biol Sci Med Sci. 2009;64(10):1049-57.
145. Song X, Mitnitski A, Rockwood K. Prevalence and 10-year outcomes of frailty in older adults in relation to deficit accumulation. Journal of the American Geriatrics Society. 2010;58(4):681-7.
146. Howlett SE. Assessment of Frailty in Animal Models. Interdisciplinary topics in gerontology and geriatrics. 2015;41:15-25.
147. Parks RJ, Fares E, Macdonald JK, Ernst MC, Sinal CJ, Rockwood K, et al. A procedure for creating a frailty index based on deficit accumulation in aging mice. J Gerontol A Biol Sci Med Sci. 2012;67(3):217-27.
148. Whitehead JC, Hildebrand BA, Sun M, Rockwood MR, Rose RA, Rockwood K, et al. A clinical frailty index in aging mice: comparisons with frailty index data in humans. J Gerontol A Biol Sci Med Sci. 2014;69(6):621-32.
149. Xie G, Wang Y, Wang X, Zhao A, Chen T, Ni Y, et al. Profiling of serum bile acids in a healthy Chinese population using UPLC-MS/MS. Journal of proteome research. 2015;14(2):850-9.
150. Frommherz L, Bub A, Hummel E, Rist MJ, Roth A, Watzl B, et al. Age-Related Changes of Plasma Bile Acid Concentrations in Healthy Adults-Results from the Cross-Sectional KarMeN Study. PloS one. 2016;11(4):e0153959.
151. Uchida K, Chikai T, Takase H, Nomura Y, Seo S, Nakao H, et al. Age-related changes of bile acid metabolism in rats. Archives of gerontology and geriatrics. 1990;10(1):37-48.
152. Fu ZD, Csanaky IL, Klaassen CD. Gender-divergent profile of bile acid homeostasis during aging of mice. PloS one. 2012;7(3):e32551.
153. Salemans JM, Nagengast FM, Tangerman A, van Schaik A, Hopman WP, de Haan AF, et al. Effect of ageing on postprandial conjugated and unconjugated serum bile acid levels in healthy subjects. Eur J Clin Invest. 1993;23(3):192-8.
154. Nagengast FM, van der Werf SD, Lamers HL, Hectors MP, Buys WC, van Tongeren JM. Influence of age, intestinal transit time, and dietary composition on fecal bile acid profiles in healthy subjects. Digestive diseases and sciences. 1988;33(6):673-8.
155. Zhang YK, Saupe KW, Klaassen CD. Energy restriction does not compensate for the reduced expression of hepatic drug-processing genes in mice with aging. Drug metabolism and disposition: the biological fate of chemicals. 2010;38(7):1122-31.
156. Bertolotti M, Gabbi C, Anzivino C, Crestani M, Mitro N, Del Puppo M, et al. Age-related changes in bile acid synthesis and hepatic nuclear receptor expression. Eur J Clin Invest. 2007;37(6):501-8.
157. Feridooni HA, Sun MH, Rockwood K, Howlett SE. Reliability of a Frailty Index Based on the Clinical Assessment of Health Deficits in Male C57BL/6J Mice. J Gerontol A Biol Sci Med Sci. 2015;70(6):686-93.
158. MacDonald JK, Pyle WG, Reitz CJ, Howlett SE. Cardiac contraction, calcium transients, and myofilament calcium sensitivity fluctuate with the estrous cycle in young adult female mice. American journal of physiology Heart and circulatory physiology. 2014;306(7):H938-53.
159. Egom EE, Vella K, Hua R, Jansen HJ, Moghtadaei M, Polina I, et al. Impaired sinoatrial node function and increased susceptibility to atrial fibrillation in mice lacking natriuretic peptide receptor C. The Journal of physiology. 2015;593(5):1127-46.

160. Yang Y, Lee LC. Dynamics and heterogeneity in the process of human frailty and aging: evidence from the U.S. older adult population. The journals of gerontology Series B, Psychological sciences and social sciences. 2010;65B(2):246-55.
161. Bansal N, Dhaliwal R, Weinstock RS. Management of diabetes in the elderly. The Medical clinics of North America. 2015;99(2):351-77.